Rab35 establishes the EHD1-association site by coordinating two distinct effectors during neurite outgrowth

Hotaka Kobayashi and Mitsunori Fukuda*

Laboratory of Membrane Trafficking Mechanisms, Department of Developmental Biology and Neurosciences, Graduate School of Life Sciences, Tohoku University, Aobayama, Aoba-ku, Sendai, Miyagi 980-8578, Japan

*Author for correspondence (nori@m.tohoku.ac.jp)

Accepted 18 March 2013
Journal of Cell Science 126, 2424–2435

doi: 10.1242/jcs.117846

Summary

Endocytic recycling is a process in which molecules that have been internalized are recycled back to the plasma membrane, and although it is crucial for regulating various cellular events, the molecular nexus underlying this process remains poorly understood. Here we report a molecular link between two gatekeepers for endocytic recycling, the molecular switch Rab35 and the molecular scissors EHD1, that is mediated by two distinct Rab35 effectors during neurite outgrowth of PC12 cells. Rab35 forms a tripartite complex with MICAL-L1 and centaurin-β2/ACAP2 and recruits them to perinuclear Arf6-positive endosomes in response to nerve growth factor stimulation. MICAL-L1 and centaurin-β2 then cooperatively recruit EHD1 to the same compartment by functioning as a scaffold for EHD1 and as an inactivator of Arf6, respectively. We propose that Rab35 regulates the formation of an EHD1-association site on Arf6-positive endosomes by integrating the functions of two distinct Rab35 effectors for successful neurite outgrowth.

Key words: Rab35, Centaurin-β2, ACAP2, Arf6, MICAL-L1, EHD1, Endocytic recycling, Neurite outgrowth

Introduction

The membrane proteins and lipids that have been internalized by endocytosis are first transported to early endosomes/sorting endosomes, and they then proceed to either a degradation pathway (to lysosomes) or a recycling pathway (to the plasma membrane) (Maxfield and McGraw, 2004; Sorkin and von Zastrow, 2009; Grant and Donaldson, 2009; Scita and Di Fiore, 2010). In many cases, cargos that are recycled back to the plasma membrane are transported from early endosomes to recycling endosomes, which are distributed in the perinuclear area, especially around the centrosome, and then returned to the plasma membrane (van Ijzendoorn, 2006). This series of membrane trafficking in the recycling process is often referred to as endocytic recycling and plays a crucial role not only in the reuse of receptor molecules but in the remodeling of membrane components of the plasma membrane through polarized recycling, which is required for various cellular events, including cell migration, cytokinesis, and neurite outgrowth (de Curtis, 2001; Montagnac and Chavrier, 2008; Sann et al., 2009). Some regulators of endocytic recycling have been identified in the literature, but their precise molecular mechanisms, especially how they are orchestrated functionally, are largely unknown.

EHD1 is one of the gatekeepers for endocytic recycling that belongs to the dynamin-like C-terminal Eps15 homology domain (EHD) protein family (Naslavsky and Caplan, 2011). EHD1 localizes to recycling endosomes and promotes membrane trafficking of various receptors, including the transferrin receptor, major histocompatibility complex (MHC) class I, and β1-integrin, mainly from recycling endosomes to the plasma membrane presumably by functioning as molecular scissors that facilitate fission of vesicles from recycling endosomes via its ATPase activity (Lin et al., 2001; Caplan et al., 2002; Jović et al., 2007). Association of EHD1 with tubular endosomal compartments (a kind of recycling endosomes in certain cell lines, e.g. HeLa cells) is achieved by MICAL-L1 and phosphatidylinositol 4-phosphate (PtdIns4*P*) (Jović et al., 2009; Sharma et al., 2009). MICAL-L1 recruits EHD1 to MICAL-L1-positive recycling endosomes through interaction with the Eps15 homology (EH) domain of EHD1, which interacts with an Asn-Pro-Phe (NPF) motif of MICAL-L1. The EH domain also binds to PtdIns4*P* on recycling endosomes and this binding activity is also required for successful recruitment of EHD1 to the same compartment. Interestingly, the amount of PtdIns4*P* has been shown to be regulated by the Arf family small GTPase Arf6, which localizes to recycling endosomes and inhibits the association of EHD1 with the endosomes (Donaldson, 2003; van Ijzendoorn, 2006; Jović et al., 2009). However, the functional relationships between MICAL-L1 and Arf6 and their upstream regulator(s) for successful recruitment of EHD1 to recycling endosomes remain poorly understood.

Rab family small GTPases function as molecular switches that drive or stop membrane trafficking by cycling between a GTP-bound active state (ON state) and a GDP-bound inactive state (OFF state) (Zerial and McBride, 2001; Stenmark, 2009). The cycling is controlled by two regulatory factors, a guanine nucleotide exchange factor (GEF), which activates Rabs, and a GTPase-activating protein (GAP), which inactivates them (Barr and Lambright, 2010). Active Rabs localize to various organelles or vesicles and promote their trafficking by recruiting specific effector molecules (Fukuda, 2008). Rab35

Journal of Cell Science

is known to function as a molecular switch for endocytic recycling and to regulate cytokinesis, phagocytosis and neurite outgrowth (Kouranti et al., 2006; Chevallier et al., 2009; Shim et al., 2010; Kobayashi and Fukuda, 2012). We recently reported finding that Rab35 localizes to perinuclear Arf6-positive endosomes and recruits Arf6-GAP centaurin-β2/ACAP2, as a Rab35 effector, to the endosomes, where it inactivates Arf6 during neurite outgrowth (Kobayashi and Fukuda, 2012), but the entire series of events by which Rab35 regulates neurite outgrowth remains to be identified.

Here we report that Rab35 regulates the formation of an EHD1-association site by recruiting two distinct Rab35 effector molecules, MICAL-L1 and centaurin-β2, during neurite outgrowth. We found that active Rab35 coordinates MICAL-L1 and centaurin-β2 at Arf6-positive endosomes in response to nerve growth factor (NGF) stimulation, which induces neurite

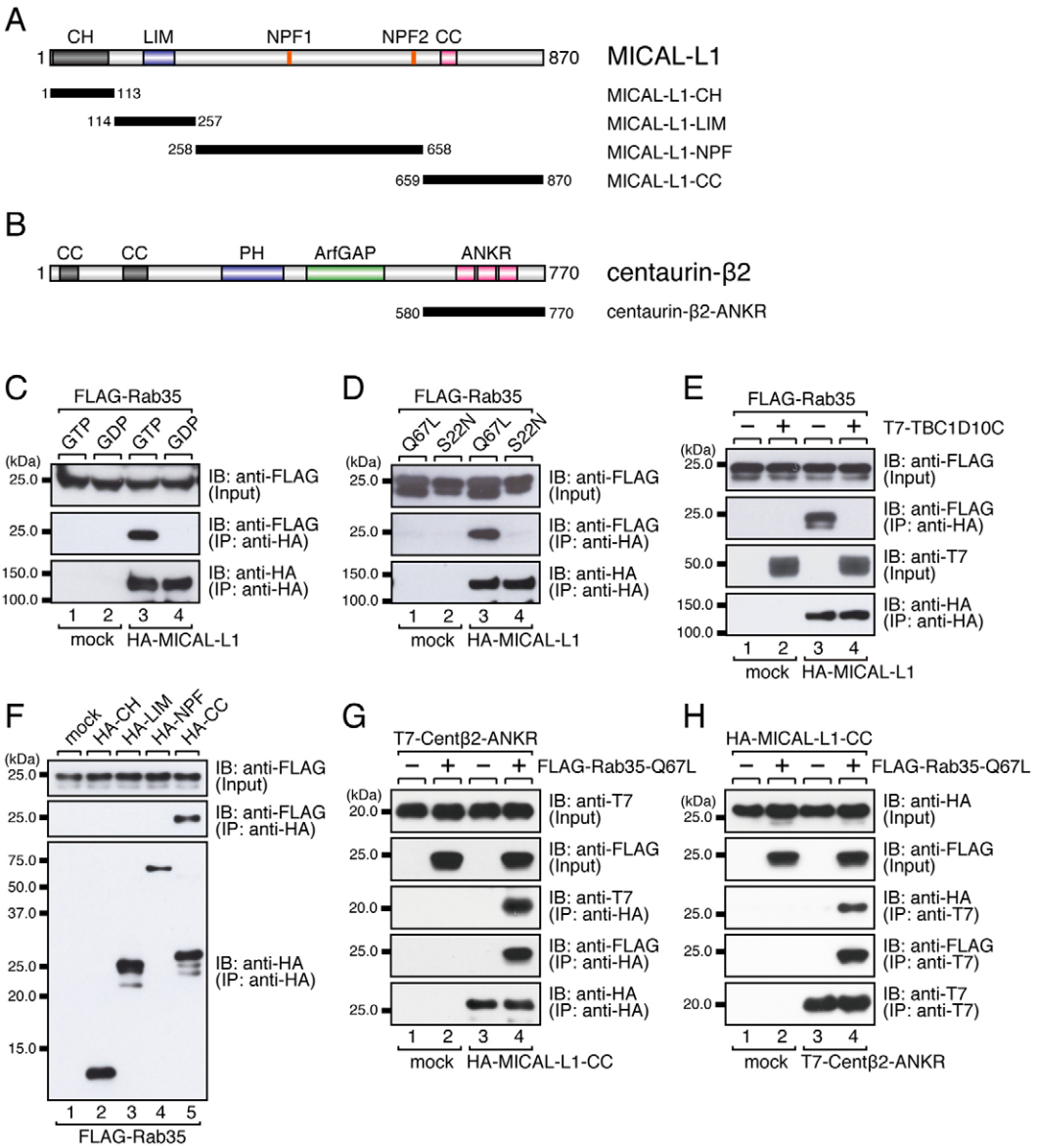

Fig. 1. Active Rab35 forms a tripartite complex with MICAL-L1 and centaurin-β2. (**A**,**B**) Schematic representation of the domain structure of MICAL-L1 (A) and of centaurin-β2 (Centβ2; B). The truncated mutants of MICAL-L1 and of Centβ2 used in the co-immunoprecipitation assays in C–H are represented by solid lines. CH, calponin homology domain; LIM, LIM domain; NPF, Asn-Pro-Phe motif; CC, coiled-coil domain; PH, pleckstrin homology domain; ArfGAP, Arf-GAP domain; and ANKR, ankyrin-repeat domain. (**C**) GTP-dependent interaction between MICAL-L1 and Rab35. Beads coupled with HA–MICAL-L1 were incubated with GTP-loaded FLAG–Rab35 or GDP-loaded FLAG–Rab35. (**D**) Interaction between MICAL-L1 and Rab35-Q67L. Beads coupled with HA–MICAL-L1 were incubated with FLAG–Rab35-Q67L or FLAG–Rab35-S22N. (**E**) Inhibition of the interaction between MICAL-L1 and Rab35 by a Rab35-specific GAP, TBC1D10C. Beads coupled with HA–MICAL-L1 were incubated with FLAG–Rab35 alone or with FLAG–Rab35 together with T7–TBC1D10C. (**F**) Identification of MICAL-L1-CC as a Rab35-binding region. Beads coupled with HA–MICAL-L1-CH, HA–MICAL-L1-LIM, HA–MICAL-L1-NPF or HA–MICAL-L1-CC were incubated with GTP-loaded FLAG–Rab35. (**G**,**H**) Rab35-Q67L mediates an indirect interaction between MICAL-L1-CC and Centβ2-ANKR. Beads coupled with HA–MICAL-L1-CC were incubated with T7–Centβ2-ANKR (G), and beads coupled with T7–Centβ2-ANKR were incubated with HA–MICAL-L1-CC (H), in the absence or presence of FLAG–Rab35-Q67L.

outgrowth of PC12 cells. The recruited MICAL-L1 and centaurin-β2 then recruit EHD1 to the same compartment by functioning as a scaffold factor for EHD1 and as an inactivator of Arf6, respectively. Our findings reveal a novel molecular nexus consisting of these five endocytic recycling factors, i.e. Rab35, centaurin-β2, Arf6, MICAL-L1 and EHD1, that are required for successful neurite outgrowth.

Results

Active Rab35 forms a tripartite complex with MICAL-L1 and centaurin-β2

We have previously shown that active Rab35 and its effector centaurin-β2 promote neurite outgrowth of neuronal cells (Kanno et al., 2010; Fukuda et al., 2011; Kobayashi and Fukuda, 2012). To identify additional Rab35 effector molecules involved in neurite outgrowth, we focused on MICAL-L1 (Fig. 1A), which we previously identified as a novel Rab35-binding protein by yeast two-hybrid screening (Fukuda et al., 2008), because MICAL-L1 had also been identified as a key molecule for endocytic recycling, the process required for neurite outgrowth (Sann et al., 2009; Sharma et al., 2009). To determine whether MICAL-L1 actually functions as a Rab35 effector, we first performed co-immunoprecipitation assays to investigate whether MICAL-L1 preferentially interacts with active Rab35. The results showed that MICAL-L1 specifically interacted with GTP-bound Rab35 and that it did not interact with GDP-bound Rab35 (Fig. 1C). Similarly, MICAL-L1 specifically interacted with Rab35-Q67L, a constitutively active mutant of Rab35, but it did not interact with Rab35-S22N, a constitutively negative mutant of Rab35 (Fig. 1D). Moreover, the interaction between MICAL-L1 and Rab35 was almost completely disrupted by coexpression of TBC1D10C (Fig. 1E), a Rab35-GAP (Patino-Lopez et al., 2008), indicating that MICAL-L1 specifically interacts with active Rab35. Because MICAL-L1 contains at least five putative protein-protein interaction domains/motifs (Fig. 1A), i.e. a calponin homology (CH) domain, a Lin-11/Isl-1/Mec-3 (LIM) domain, two NPF motifs, and a coiled-coil (CC) domain, we attempted to map the Rab35-binding region of MICAL-L1 by co-immunoprecipitation assays with a series of MICAL-L1 deletion mutants (Fig. 1A). The results of the deletion analysis indicated that the MICAL-L1-CC specifically interacted with Rab35 (Fig. 1F). The GTP-dependent interaction between MICAL-L1-CC and Rab35 was also observed when purified recombinant proteins were used, the same as the interaction between centaurin-β2 and Rab35 (supplementary material Fig. S1A–C).

Because we had previously shown that the interaction between active Rab35 and centaurin-β2 via its ankyrin repeat (ANKR) domain is essential for neurite outgrowth (Fig. 1B) (Kanno et al., 2010), we proceeded to perform co-immunoprecipitation assays to determine whether MICAL-L1 is able to interact with Rab35 without affecting the interaction between Rab35 and centaurin-β2. The results showed that MICAL-L1-CC co-immunoprecipitated centaurin-β2-ANKR through Rab35-Q67L (Fig. 1G), and vice versa (Fig. 1H), indicating that Rab35, MICAL-L1 and centaurin-β2 form a tripartite complex.

Rab35 recruits MICAL-L1 to Arf6-positive endosomes

We next performed immunofluorescence analyses to investigate the subcellular localization of MICAL-L1 in PC12 cells before and after NGF stimulation. Consistent with the results of our previous study (Kobayashi and Fukuda, 2012), both Rab35 and centaurin-β2 were recruited to perinuclear Arf6-positive endosomes in response to NGF stimulation, and, interestingly,

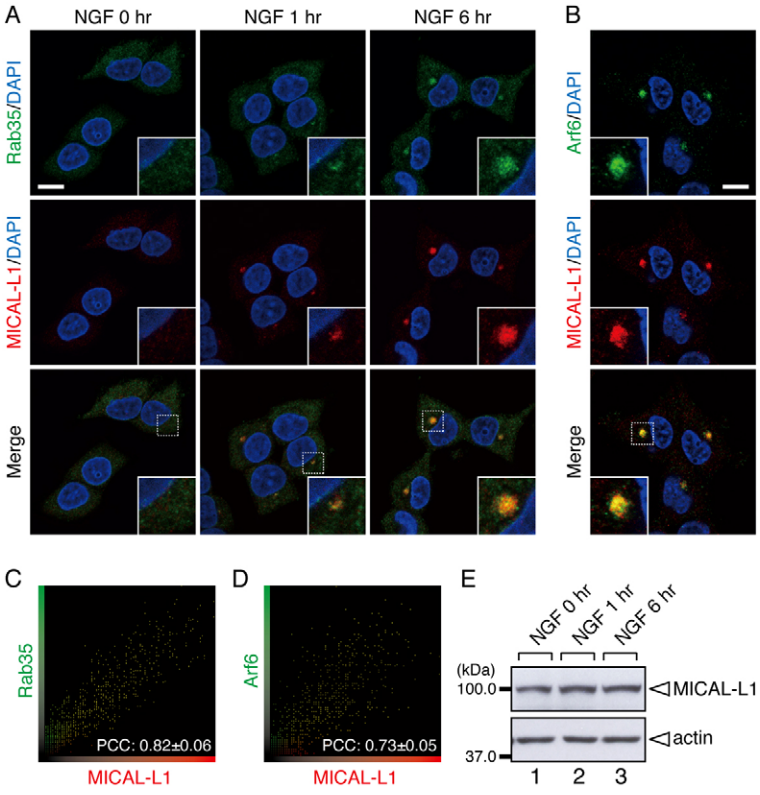

Fig. 2. Rab35 and MICAL-L1 are concomitantly recruited to Arf6-positive endosomes in response to NGF stimulation. (**A**) Accumulation of Rab35 and MICAL-L1 in the perinuclear area of PC12 cells in response to NGF stimulation. After NGF stimulation for 0 hours (no NGF treatment), 1 hour and 6 hours, PC12 cells were fixed and stained with anti-Rab35 antibody, anti-MICAL-L1 antibody and DAPI. (**B**) Colocalization between Arf6 and MICAL-L1 in PC12 cells. PC12 cells were fixed and stained with anti-Arf6 antibody, anti-MICAL-L1 antibody and DAPI after NGF stimulation for 6 hours. The insets in A and B show magnified views of the boxed areas. Scale bars: 10 μm. (**C**,**D**) The intensity-scatter plot of Rab35 signals versus MICAL-L1 signals (C) and of Arf6 signals versus MICAL-L1 signals (D) in PC12 cells after NGF stimulation for 6 hours. Pearson's correlation coefficient (PCC) value (mean ± s.d.) for the relationship between them is shown at the bottom (n=30 from three independent experiments). (**E**) Unaltered expression of MICAL-L1 in PC12 cells during NGF stimulation. After NGF stimulation for 0 hours, 1 hour and 6 hours, cell lysates of PC12 cells were immunoblotted with anti-MICAL-L1 antibody and anti-actin antibody.

MICAL-L1 was also concomitantly recruited to the same compartment and highly colocalized with both Rab35 and centaurin-β2 (Fig. 2A–D and supplementary material Fig. S2; Pearson's correlation coefficient (PCC), 0.82±0.06 for Rab35, 0.92±0.02 for centaurin-β2 and 0.73±0.05 for Arf6). The increase in signals in the perinuclear area was unlikely to be attributable to the increased expression of MICAL-L1 in response to NGF stimulation, because its level of expression before and after NGF stimulation was similar (Fig. 2E).

Since MICAL-L1 has the ability to bind active Rab35, we hypothesized that MICAL-L1 is also recruited to Arf6-positive endosomes by Rab35, the same as centaurin-β2 is (Kobayashi and Fukuda, 2012). To test our hypothesis, we investigated the subcellular localization of MICAL-L1 in the Rab35-depleted PC12 cells in the presence of NGF stimulation. As expected, the perinuclear MICAL-L1 signals dramatically decreased in Rab35-depleted PC12 cells (Fig. 3A,B; 19.2±3.9% of control cells), indicating that Rab35 is actually required for the perinuclear recruitment of MICAL-L1. By contrast, depletion of MICAL-L1 had no effect on the perinuclear localization of Rab35 (Fig. 3D,E; 116.8±14.9% of control cells) or expression of Rab35 (Fig. 3F). Since the level of expression of MICAL-L1 was unaltered by the depletion of Rab35 (Fig. 3C), the MICAL-L1 in Rab35-depleted PC12 cells is likely to have been dispersed from the perinuclear compartments into the cytosol or other membrane compartments. Interestingly, depletion of MICAL-L1 (or centaurin-β2) slightly decreased the perinuclear signals of centaurin-β2 (or MICAL-L1; supplementary material Fig. S3; ~70% of control cells), suggesting that MICAL-L1 partly stabilizes the perinuclear localization of centaurin-β2, and vice versa. We also analyzed the localization of MICAL-L1 deletion mutants in PC12 cells in the presence of NGF stimulation, and the results confirmed that the active Rab35-binding CC domain is responsible for the perinuclear localization of MICAL-L1, because MICAL-L1-CC, but not MICAL-L1-ΔCC, was localized to the perinuclear area (Fig. 3G). If Rab35 primarily determines the perinuclear localization of MICAL-L1, then ectopically expressing Rab35 at the plasma membrane by using a plasma membrane-targeting sequence (CAAX) of K-Ras (Hancock et al., 1991) should alter the subcellular localization of MICAL-L1-CC. As expected, MICAL-L1-CC was dramatically translocated to the plasma membrane in Rab35-Q67L–CAAX-expressing PC12 cells, but it was not translocated in Rab35-S22N–CAAX-expressing PC12 cells (Fig. 3H). Consistent with the finding that active Rab35 forms a tripartite complex with MICAL-L1 and centaurin-β2 (Fig. 1G,H and supplementary material Fig. S1), Rab35-Q67L–CAAX also induced dramatic translocation of centaurin-β2 to the plasma membrane (supplementary material Fig. S4). We therefore concluded that MICAL-L1 is recruited to Arf6-positive endosomes through interaction with Rab35, the same as centaurin-β2 is (Kobayashi and Fukuda, 2012).

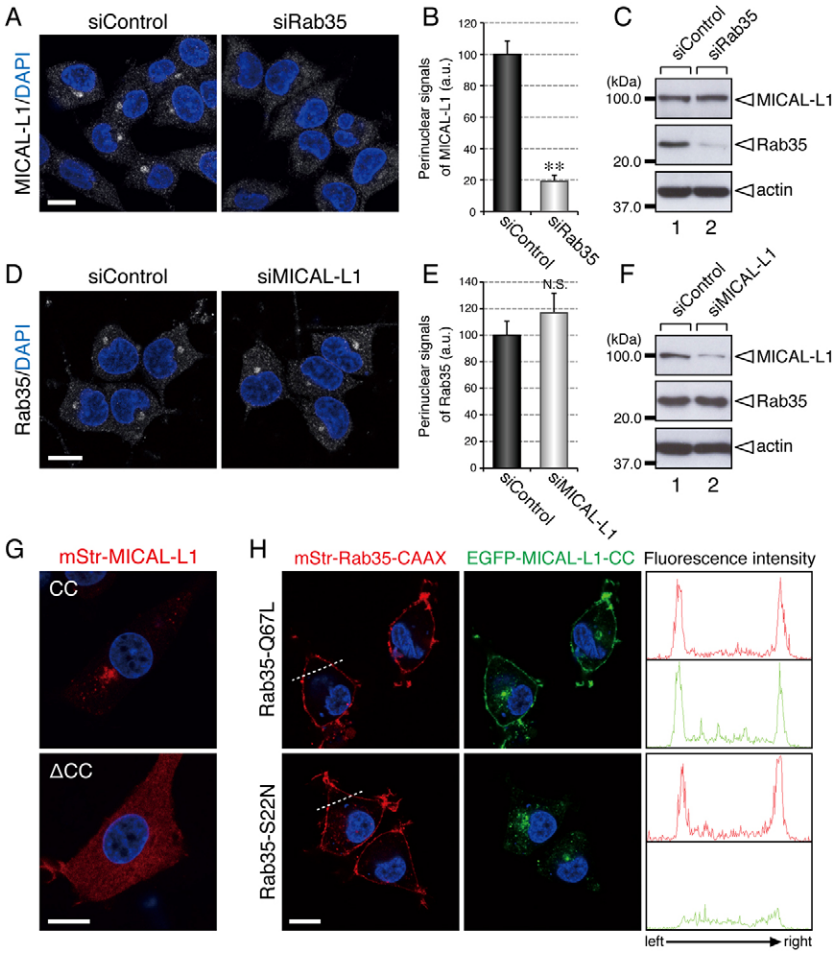

Fig. 3. Rab35 primarily determines the localization of MICAL-L1. (**A**,**B**) Disappearance of MICAL-L1 signals from the perinuclear area of Rab35-depleted PC12 cells. (A) PC12 cells transfected with control siRNA (siControl) or *Rab35* siRNA (siRab35) were fixed and stained with anti-MICAL-L1 antibody and DAPI after NGF stimulation for 6 hours. (B) Perinuclear MICAL-L1 signals (mean and s.e.m.; arbitrary units, a.u.) of siControl-treated and siRab35-treated PC12 cells (n=60 from three independent experiments). (**C**) Unaltered expression of MICAL-L1 in Rab35-depleted PC12 cells. Cell lysates of PC12 cells treated with either siControl or siRab35 were immunoblotted with anti-MICAL-L1 antibody, anti-Rab35 antibody and anti-actin antibody. (**D**,**E**) Perinuclear localization of Rab35 is independent of MICAL-L1 in PC12 cells. (D) PC12 cells transfected with siControl or siMICAL-L1 were fixed and stained with anti-Rab35 antibody and DAPI after NGF stimulation for 6 hours. (E) Perinuclear Rab35 signals (mean and s.e.m.; arbitrary units, a.u.) of siControl-treated and siMICAL-L1-treated PC12 cells (n=60 from three independent experiments). N.S., not significant in comparison with the control cells (Student's unpaired t-test). (**F**) Unaltered expression of Rab35 in MICAL-L1-depleted PC12 cells. Cell lysates of PC12 cells treated with either siControl or siMICAL-L1 were immunoblotted in the same manner as described in C. (**G**) Perinuclear localization of MICAL-L1 is mediated by its CC (Rab35-binding) domain. PC12 cells transiently expressing mStr–MICAL-L1-CC or mStr–MICAL-L1-ΔCC were fixed and stained with DAPI after NGF stimulation for 6 hours. (**H**) Translocation of MICAL-L1-CC to the plasma membrane in response to expression of plasma membrane-localized Rab35-Q67L–CAAX. PC12 cells transiently expressing EGFP–MICAL-L1-CC together with either mStr–Rab35-Q67L–CAAX or mStr–Rab35-S22N–CAAX were fixed and stained with DAPI after NGF stimulation for 6 hours. Fluorescence intensity along the dashed lines is shown at the right. Scale bars: 10 μm.

MICAL-L1 functions as an essential mediator of neurite outgrowth

We adopted the following three independent approaches to determine whether MICAL-L1 actually functions as a downstream effector of Rab35 during neurite outgrowth. The first approach was to knock down MICAL-L1 in PC12 cells (Fig. 4C) and evaluate its effect on neurite outgrowth. The same as the depletion of Rab35 or centaurin-β2 had (Kobayashi and Fukuda, 2012), depletion of MICAL-L1 induced a dramatic reduction in the neurite length of PC12 cells (Fig. 4A,B). The second approach was to use a dominant negative method to examine the importance of the interaction between Rab35 and MICAL-L1 during neurite outgrowth. We did so by overexpressing MICAL-L1-CC, which had been found to disrupt the interaction between Rab35 and MICAL-L1 *in vitro* (Fig. 4F), in PC12 cells and evaluating its effect on neurite outgrowth. As shown in Fig. 4D,E, overexpression of MICAL-L1-CC in PC12 cells caused a dramatic reduction in neurite length. The third approach was to investigate the possible involvement of MICAL-L1 in Rab35-Q67L-dependent neurite outgrowth of PC12 cells (Kanno et al., 2010; Kobayashi and Fukuda, 2012) as a means of determining whether MICAL-L1 is required for active Rab35-dependent neurite outgrowth. The results showed that knockdown of MICAL-L1 strongly inhibited Rab35-Q67L-promoted neurite outgrowth (Fig. 4G,H). Taken together, these results obtained by these three approaches indicated that MICAL-L1 functions as a novel Rab35 effector during neurite outgrowth, the same as centaurin-β2 does.

Rab35 anchors EHD1 to Arf6-positive endosomes through MICAL-L1

How does Rab35 regulate neurite outgrowth by recruiting MICAL-L1 to Arf6-positive endosomes? To answer this question, we focused on another key factor in endocytic recycling, EHD1, because MICAL-L1 has been reported to be a scaffold protein for EHD1 (Sharma et al., 2009). Since Rab35 positively regulates the localization of MICAL-L1 (Fig. 3), it seemed very possible that Rab35 recruits EHD1 to Arf6-positive endosomes through MICAL-L1 during neurite outgrowth. To investigate this possibility, we performed immunofluorescence

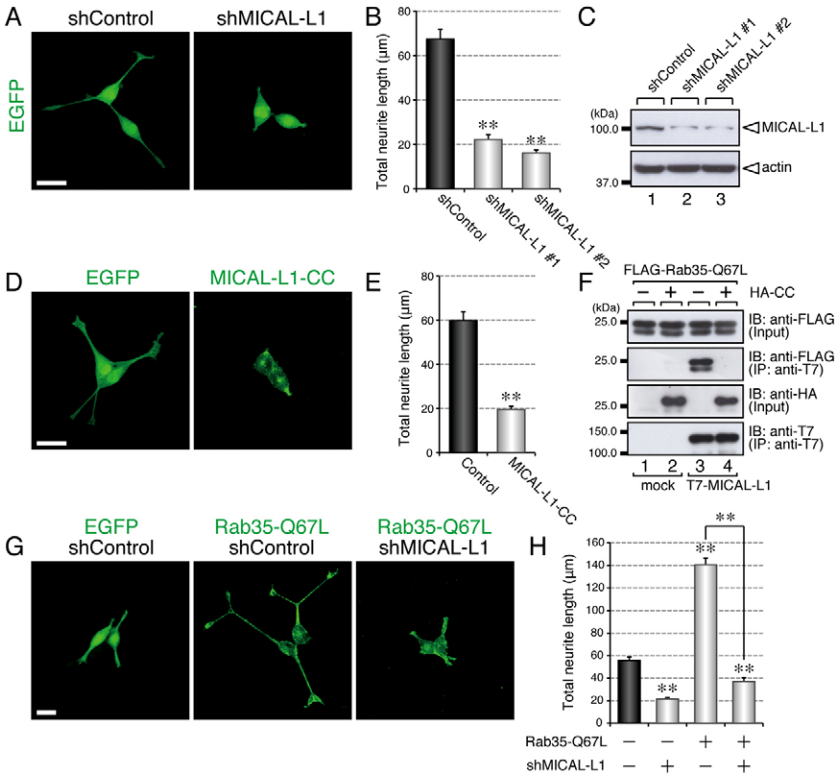

Fig. 4. MICAL-L1 is an essential mediator of neurite outgrowth. (**A**,**B**) Inhibition of neurite outgrowth by depletion of endogenous MICAL-L1. (A) Typical images of control shRNA (shControl)-treated and *MICAL-L1* shRNA (shMICAL-L1)-treated PC12 cells after NGF stimulation for 36 hours. (B) Total neurite length (mean and s.e.m.) of shControl-treated, shMICAL-L1 #1-treated and shMICAL-L1 #2-treated PC12 cells (n>100). (**C**) Reduced expression of MICAL-L1 in shMICAL-L1-treated PC12 cells. Cell lysates of PC12 cells treated with shControl, shMICAL-L1 #1 or shMICAL-L1 #2 were immunoblotted with anti-MICAL-L1 antibody and anti-actin antibody. (**D**,**E**) Inhibition of neurite outgrowth by overexpression of MICAL-L1-CC. (D) Typical images of EGFP-expressing and EGFP–MICAL-L1-CC-expressing PC12 cells after NGF stimulation for 36 hours. (E) Total neurite length (mean and s.e.m.) of EGFP-expressing and EGFP–MICAL-L1-CC-expressing PC12 cells (n>100). (**F**) Disruption of the interaction between Rab35-Q67L and MICAL-L1 by MICAL-L1-CC. Beads coupled with T7–MICAL-L1 were incubated with FLAG–Rab35-Q67L in the absence or presence of HA–MICAL-L1-CC. (**G**,**H**) Inhibition of Rab35-Q67L-enhanced neurite outgrowth by depletion of endogenous MICAL-L1. (G) Typical images of EGFP + shControl-expressing, EGFP–Rab35-Q67L + shControl-expressing and EGFP–Rab35-QL + shMICAL-L1-expressing PC12 cells after NGF stimulation for 36 hours. Scale bars: 30 μm (A,D,G). (H) Total neurite length (mean and s.e.m.) of EGFP + shControl-expressing, EGFP + shMICAL-L1-expressing, EGFP–Rab35-Q67L + shControl-expressing and EGFP–Rab35-Q67L + shMICAL-L1-expressing PC12 cells (n>100).

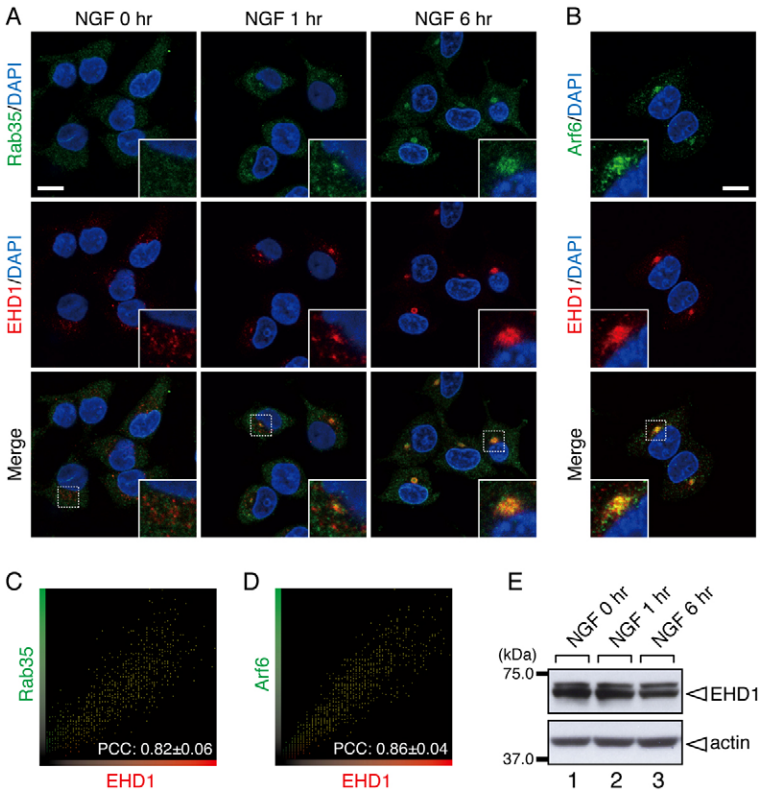

Fig. 5. Rab35 and EHD1 are concomitantly recruited to Arf6-positive endosomes in response to NGF stimulation. (**A**) Accumulation of Rab35 and EHD1 in the perinuclear area of PC12 cells in response to NGF stimulation. After NGF stimulation for 0 hours (no NGF treatment), 1 hour and 6 hours, PC12 cells were fixed and stained with anti-Rab35 antibody, anti-EHD1 antibody and DAPI. (**B**) Colocalization between Arf6 and EHD1 in PC12 cells. PC12 cells were fixed and stained with anti-Arf6 antibody, anti-EHD1 antibody and DAPI after NGF stimulation for 6 hours. The insets in A and B show magnified views of the boxed areas. Scale bars: 10 μm. (**C**,**D**) Intensity-scatter plots of Rab35 signals versus EHD1 signals (C) and of Arf6 signals versus EHD1 signals (D) in PC12 cells after NGF stimulation for 6 hours. PCC value (means ± s.d.) for the relationship between them is shown at the bottom (n=30 from three independent experiments). (**E**) Unaltered expression of EHD1 in PC12 cells during NGF stimulation. After NGF stimulation for 0 hours, 1 hour and 6 hours, cell lysates of PC12 cells were immunoblotted with anti-EHD1 antibody and anti-actin antibody.

analyses to determine the subcellular localization of EHD1 in PC12 cells before and after NGF stimulation. Interestingly, EHD1 was found to also have accumulated in the perinuclear area and to have colocalized with Arf6 in response to NGF stimulation (Fig. 5A,B,D; PCC, 0.86±0.04), the same as Rab35 and MICAL-L1 had. It was particularly noteworthy that EHD1 was closely colocalized with both Rab35 and MICAL-L1 (Fig. 5A,C; supplementary material Fig. S5A,C; PCC, 0.82±0.06 for Rab35 and 0.74±0.04 for MICAL-L1). The same as in the increase in MICAL-L1 signals (Fig. 2E), the increase in EHD1 signals in the perinuclear area was also unlikely to be attributable to the increased expression of EHD1 in response to NGF stimulation (Fig. 5E). Such perinuclear recruitment of EHD1 requires both Rab35 and MICAL-L1, because the perinuclear EHD1 signals dramatically decreased in both Rab35-depleted PC12 cells and MICAL-L1-depleted PC12 cells (Fig. 6A,B; 19.8±5.4% in Rab35-depleted cells and 36.1±7.9% in MICAL-L1-depleted cells, in comparison with the control cells). Under these experimental conditions, neither Rab35 depletion nor MICAL-L1 depletion affected the level of expression of EHD1 (Fig. 6C,D).

We then performed co-immunoprecipitation assays to investigate whether Rab35 associates with EHD1 through MICAL-L1. The results clearly showed that active Rab35 was co-purified with EHD1 only in the presence of MICAL-L1 (Fig. 6E), indicating active Rab35 indirectly interacts with EHD1 through MICAL-L1. To confirm that the Rab35–MICAL-L1 interaction regulates the localization of EHD1, we ectopically expressed active Rab35 at the plasma membrane by using the CAAX-tag as described above and analyzed the subcellular localization of EHD1. As expected, EHD1 was clearly translocated to the plasma membrane in the Rab35-Q67L–CAAX- and MICAL-L1-expressing PC12 cells (Fig. 6G, left panels). By contrast, expression of Rab35-Q67L–CAAX together with MICAL-L1-ΔCC (Rab35-binding-deficient) or with MICAL-L1-ΔNPF (EHD1-binding-deficient; Fig. 6F) (Sharma et al., 2009) did not induce translocation of EHD1 to the plasma membrane (Fig. 6G, middle panels and right panels), indicating that both the Rab35 binding activity and the EHD1 binding activity of MICAL-L1 are required for the Rab35-Q67L-dependent localization of EHD1. These findings enabled us to conclude that the NGF-dependent perinuclear localization of EHD1 is primarily determined by Rab35 through MICAL-L1.

Another Rab35 effector, centaurin-β2, also links Rab35 and EHD1

Because centaurin-β2 functions as a GAP for Arf6 (Jackson et al., 2000), which also regulates the localization of EHD1 in HeLa cells (Jović et al., 2009), we further hypothesized that centaurin-β2 also regulates the connection between Rab35 and EHD1 during neurite outgrowth of PC12 cells. To test our hypothesis, we first investigated the subcellular localization of centaurin-β2 and EHD1 in NGF-stimulated PC12 cells by immunofluorescence analyses, and the results showed that centaurin-β2 was closely colocalized with EHD1 (supplementary material Fig. S5B,D; PCC, 0.91±0.04). We then investigated the subcellular localization of EHD1 in centaurin-β2-depleted PC12 cells in the presence of NGF stimulation. Interestingly, the perinuclear EHD1 signals dramatically decreased in centaurin-β2-depleted PC12 cells (Fig. 7A,D; 16.8±5.7% of control cells), indicating that centaurin-β2 is actually required for the perinuclear recruitment of EHD1. Most importantly, the effect of knockdown of centaurin-β2 on the recruitment of EHD1 was rescued by re-expression of an siRNA-resistant (SR) form of centaurin-β2, but not by re-expression of centaurin-β2^{SR}-R442Q (Jackson et al., 2000), an

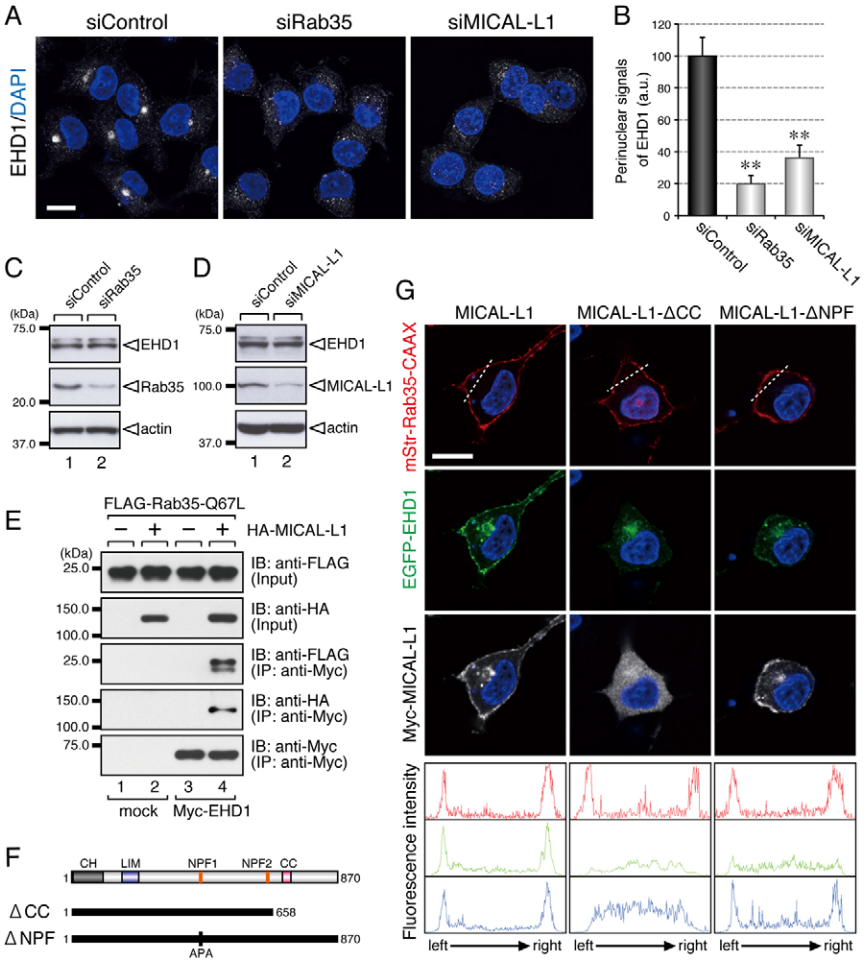

Fig. 6. Rab35 determines the perinuclear localization of EHD1 through MICAL-L1. (**A**,**B**) Disappearance of EHD1 signals from the perinuclear area in Rab35-depleted PC12 cells and MICAL-L1-depleted PC12 cells. (A) PC12 cells transfected with control siRNA (siControl), *Rab35* siRNA (siRab35) or *MICAL-L1* siRNA (siMICAL-L1) were fixed and stained with anti-EHD1 antibody and DAPI after NGF stimulation for 6 hours. (B) Perinuclear EHD1 signals (mean and s.e.m.; a.u., arbitrary units) of siControl-treated, siRab35-treated and siMICAL-L1-treated cells ($n=60$ from three independent experiments). (**C**,**D**) Unaltered expression of EHD1 in Rab35-depleted PC12 cells and MICAL-L1-depleted PC12 cells. Cell lysates of PC12 cells treated with siControl, siRab35 or siMICAL-L1 were immunoblotted with anti-EHD1 antibody, anti-Rab35 antibody (C), anti-MICAL-L1 antibody (D) and anti-actin antibody. (**E**) Indirect interaction between Rab35-Q67L and EHD1 through MICAL-L1. Beads coupled with Myc–EHD1 were incubated with FLAG–Rab35-Q67L in the absence or presence of HA–MICAL-L1. (**F**) Schematic representation of the two deletion mutants of MICAL-L1. MICAL-L1-ΔCC lacks the Rab35-binding CC domain. MICAL-L1-ΔNPF contains APA (Ala-Pro-Ala) mutations in the first NPF motif, which is responsible for EHD1 binding. (**G**) Translocation of EHD1 to the plasma membrane by expression of Rab35-Q67L–CAAX and MICAL-L1. PC12 cells transiently expressing EGFP–EHD1 and mStr–Rab35-Q67L–CAAX together with Myc–MICAL-L1, Myc–MICAL-L1-ΔCC or Myc–MICAL-L1-ΔNPF were fixed and stained with anti-Myc tag antibody and DAPI after NGF stimulation for 6 hours. Fluorescence intensity along the dashed lines is shown at the bottom. Scale bars: 10 μm.

Arf6-GAP activity-deficient mutant in which Arg 442 of centaurin β2 is replaced with Gln (Fig. 7B–D; 142.3±16.2% in centaurin-β2-expressing cells and 18.7±6.6% in centaurin-β2-R442Q-expressing cells, in comparison with the control cells). Moreover, overexpression of Arf6-Q67L, a constitutively active mutant of Arf6, also caused a dramatic reduction in the perinuclear EHD1 signals in NGF-stimulated PC12 cells (Fig. 7E; 28.5±10.1% of control cells). The level of EHD1 expression was unaltered by the depletion of centaurin-β2 or by the overexpression of Arf6-Q67L (Fig. 7F,G). We therefore concluded that inactivation of Arf6 by centaurin-β2 is essential for the recruitment of EHD1.

Because ectopic expression of Rab35 at the plasma membrane induced translocation of EHD1 to the plasma membrane (Fig. 6G), we proceeded to investigate whether the translocation would be inhibited by activation of Arf6 at the plasma membrane. To do so, we expressed Arf6-Q67L at the plasma membrane by using the CAAX-tag and analyzed its effect on the Rab35–CAAX-dependent translocation of EHD1. The results showed that while EHD1 was translocated to the plasma membrane in Rab35-Q67L–CAAX-expressing PC12 cells (Fig. 7H, top panels), its translocation was dramatically inhibited by coexpression of Arf6-Q67L–CAAX at the plasma membrane (Fig. 7H, bottom panels), indicating that inactivation of Arf6 is essential for the Rab35- and MICAL-L1-dependent recruitment of EHD1.

EHD1 functions as an essential mediator of neurite outgrowth

Finally, we investigated whether EHD1 mediates neurite outgrowth of PC12 cells. When we knocked down EHD1 in PC12 cells with specific siRNAs (Fig. 8C), the EHD1-depleted PC12 cells had dramatically shorter neurites than the control cells (Fig. 8A,B), the same as the Rab35-depleted, MICAL-L1-depleted and centaurin-β2-depleted PC12 cells (Kobayashi and Fukuda, 2012; Fig. 4A,B), indicating the functional involvement of EHD1 in neurite outgrowth of PC12 cells.

Because MICAL-L1-NPF, an EHD1-binding domain of MICAL-L1 (Sharma et al., 2009), had the ability to disrupt the interaction between MICAL-L1 and EHD1 *in vitro*, presumably by masking the MICAL-L1-binding interface of EHD1 (Fig. 8F), we overexpressed MICAL-L1-NPF and evaluated its effect on neurite outgrowth of PC12 cells. The results showed that overexpression of MICAL-L1-NPF caused a dramatic reduction in the neurite length of PC12 cells (Fig. 8D,E), suggesting the importance of the interaction between MICAL-L1 and EHD1 during neurite outgrowth. We also overexpressed the EH domain of EHD1 (EHD1-EH), a MICAL-L1 and PtdIns4*P* binding region and evaluated its effect on neurite outgrowth of PC12 cells. Again, overexpression of EHD1-EH, which presumably disrupts the interaction between EHD1 and both MICAL-L1 and PtdIns4*P*, also caused a dramatic reduction in the neurite length of PC12 cells (Fig. 8G,H). Importantly, overexpression of EHD1-EH-K483E, which lacks PtdIns4*P*

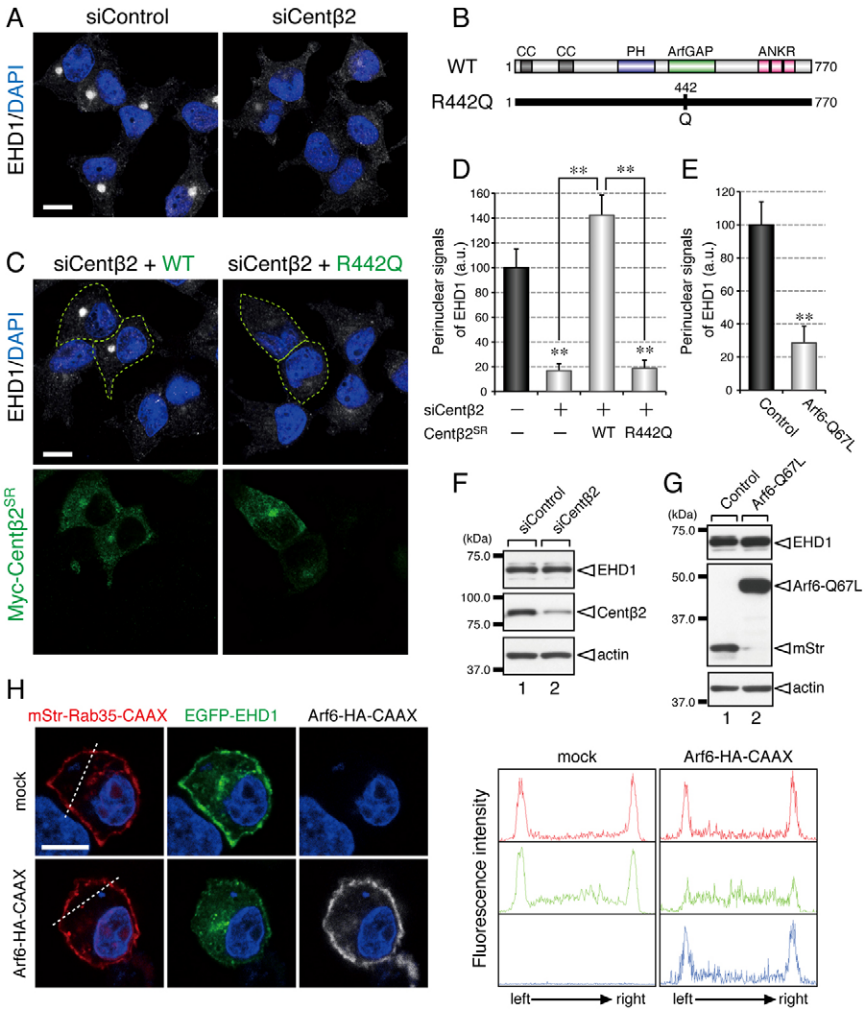

Fig. 7. Another Rab35 effector, centaurin-β2, and inactivation of Arf6 are required for perinuclear localization of EHD1. (**A**) Disappearance of EHD1 signals from the perinuclear area in centaurin-β2-depleted PC12 cells. PC12 cells transfected with either control siRNA (siControl) or centaurin-β2 siRNA (siCentβ2) were fixed and stained with anti-EHD1 antibody and DAPI after NGF stimulation for 6 hours. (**B**) Schematic representation of centaurin-β2-R442Q. Centaurin-β2-R442Q has a point mutation of the Arg 442 to Gln, which abolishes its Arf6-GAP activity. (**C**) Recovery of perinuclear EHD1 signals by re-expression of centaurin-β2, but not of centaurin-β2-R442Q, in centaurin-β2-depleted PC12 cells. PC12 cells transfected with siCentβ2 + pMyc-C1-centaurin-β2 (Myc-Centβ2) or with siCentβ2 + pMyc-C1-centaurin-β2-R442Q (Myc-Centβ2-R442Q) were fixed and stained with anti-EHD1 antibody, anti-Myc tag antibody and DAPI after NGF stimulation for 6 hours. Myc–Centβ2-expressing and Myc–Centβ2-R442Q-expressing cells are outlined by dashed lines. (**D**) Perinuclear EHD1 signals (mean and s.e.m.; a.u.,, arbitrary units) of siControl-transfected, siCentβ2-transfected, siCentβ2 + pMyc-C1-Centβ2-transfected and siCentβ2 + pMyc-C1-Centβ2-R442Q-transfected cells (n=60 from three independent experiments). (**E**) Perinuclear EHD1 signals (mean and s.e.m.; arbitrary units, a.u.) of mStr-expressing and Arf6-Q67L–mStr-expressing cells (n=60 from three independent experiments). (**F**,**G**) Unaltered expression of EHD1 in centaurin-β2-depleted (F) or Arf6-Q67L-expressing (G) PC12 cells. Cell lysates of PC12 cells treated with siControl or siCentβ2 (F) and of PC12 cells expressing mStr or Arf6-Q67L–mStr (G) were immunoblotted with anti-EHD1 antibody, anti-centaurin-β2 antibody (F), anti-red fluorescent protein antibody (G) and anti-actin antibody. (**H**) Inhibition of Rab35-Q67L–CAAX-dependent translocation of EHD1 to the plasma membrane by simultaneous expression of plasma membrane-localized Arf6-Q67L–CAAX. PC12 cells transiently expressing mStr–Rab35-Q67L–CAAX, Myc–MICAL-L1 and EGFP–EHD1 either together with or without Arf6-Q67L–HA–CAAX were fixed and stained with anti-HA tag antibody and DAPI after NGF stimulation for 6 hours. Fluorescence intensity along the dashed lines is shown at the right. Scale bars: 10 μm.

binding activity (or EHD1-EH-W485A, which lacks MICAL-L1 binding activity) (Jović et al., 2009; Sharma et al., 2009), had only a weak reducing effect on the neurite length of PC12 cells (Fig. 8G,H), suggesting the importance of the PtdIns4*P* binding activity of EHD1 to neurite outgrowth.

If EHD1 actually functions downstream of Rab35, then EHD1 should be required for active Rab35-dependent neurite outgrowth. Indeed, knockdown of EHD1 dramatically inhibited Rab35-Q67L-promoted neurite outgrowth (Fig. 8I,J). All of these findings taken together revealed a novel mechanism in which Rab35 regulates the localization of EHD1 through the recruitment of two distinct effectors, MICAL-L1 and centaurin-β2, to Arf6-positive endosomes during neurite outgrowth.

Discussion

Research conducted over the past decade has pointed to a functional relationship between Rab35 and EHD1. Genetic screening using *Caenorhabditis elegans* identified *Rab35* and

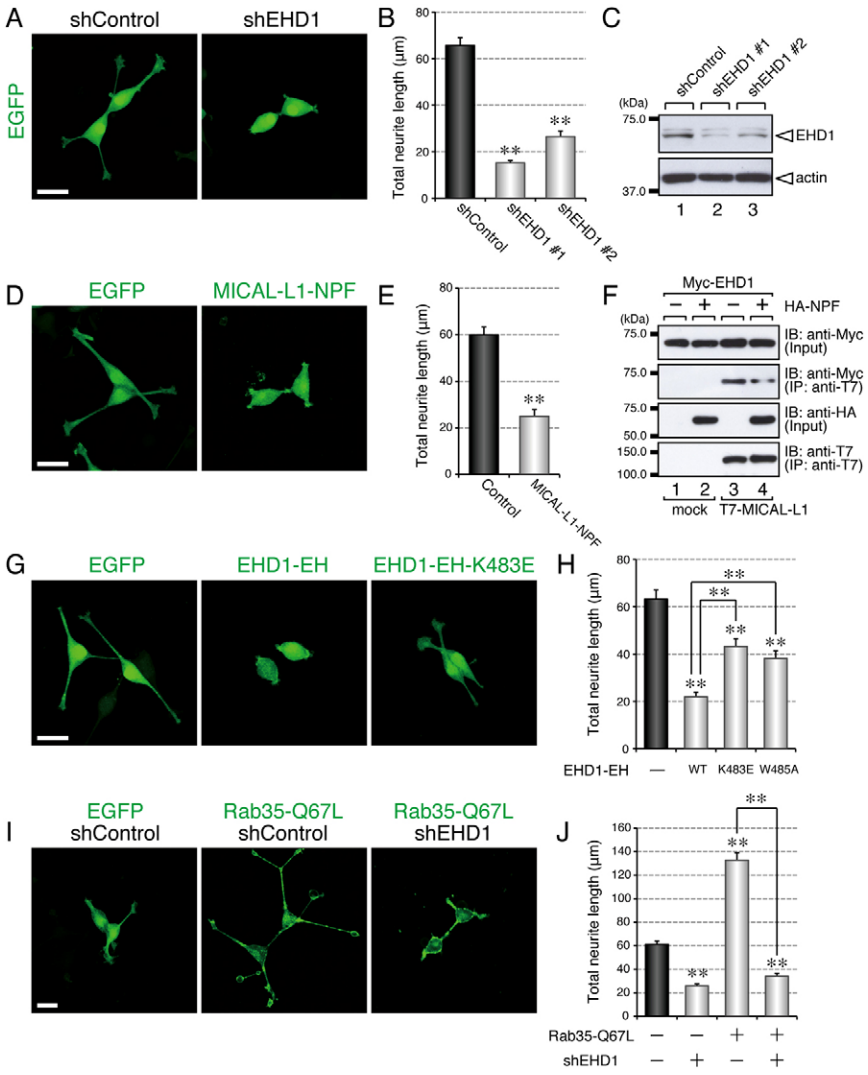

Fig. 8. EHD1 is an essential mediator of neurite outgrowth. (**A**,**B**) Inhibition of neurite outgrowth by depletion of endogenous EHD1. (A) Typical images of control shRNA (shControl)-treated and *EHD1* shRNA (shEHD1)-treated PC12 cells after NGF stimulation for 36 hours. (B) Total neurite length (mean and s.e.m.) of shControl-treated, shEHD1 #1-treated, and shEHD1 #2-treated PC12 cells (n>100). (**C**) Reduced expression of EHD1 in shEHD1-treated PC12 cells. Cell lysates of PC12 cells treated with shControl, shEHD1 #1, or shEHD1 #2 were immunoblotted with anti-EHD1 antibody and anti-actin antibody. (**D**,**E**) Inhibition of neurite outgrowth by overexpression of MICAL-L1-NPF. (D) Typical images of EGFP-expressing and EGFP–MICAL-L1-NPF-expressing PC12 cells after NGF stimulation for 36 hours. (E) Total neurite length (mean and s.e.m.) of EGFP-expressing and EGFP–MICAL-L1-NPF-expressing PC12 cells (n>100). (**F**) Disruption of the interaction between MICAL-L1 and EHD1 by MICAL-L1-NPF. Beads coupled with T7–MICAL-L1 were incubated with Myc–EHD1 in the absence or presence of HA–MICAL-L1-NPF. (**G**,**H**) Effect of EHD1-EH and its point mutants EHD1-EH-K483E and EHD1-EH-W485A on NGF-induced neurite outgrowth. (G) Typical images of EGFP-expressing, EGFP–EHD1-EH-expressing and EGFP–EHD1-EH-K483E-expressing PC12 cells after NGF stimulation for 36 hours. (H) Total neurite length (mean and s.e.m.) of EGFP-expressing, EGFP–EHD1-EH-expressing, EGFP–EHD1-EH-K483E-expressing and EGFP–EHD1-EH-W485A-expressing PC12 cells (n>100). (**I**,**J**) Inhibition of Rab35-Q67L-enhanced neurite outgrowth by depletion of endogenous EHD1. (I) Typical images of EGFP + shControl-expressing, EGFP–Rab35-Q67L + shControl-expressing and EGFP–Rab35-Q67L + shEHD1-expressing PC12 cells after NGF stimulation for 36 hours. (J) Total neurite length (mean and s.e.m.) of EGFP + shControl-expressing, EGFP + shEHD1-expressing, EGFP–Rab35-Q67L + shControl-expressing and EGFP–Rab35-Q67L + shEHD1-expressing cells (n>100). Scale bars: 30 μm.

EHD1 as *RME* (receptor-mediated endocytosis)-5 and *RME-1*, respectively (Grant and Hirsh, 1999; Lin et al., 2001; Sato et al., 2008). *RME* mutant strains exhibit a critical defect in yolk protein uptake by oocytes (Grant and Hirsh, 1999), and the uptake defects in *RME-5* and *RME-1* mutants have been shown to be attributable to defects in recycling yolk receptors back to the plasma membrane after internalization, which leads to a loss of receptors from the plasma membrane (Lin et al., 2001; Sato et al., 2008). Moreover, Allaire et al. have recently reported finding that Connecdenn, a Rab35-GEF, is required for the localization of EHD1 at recycling endosomes, suggesting that Rab35 functions upstream of EHD1 in endocytic recycling (Allaire et al., 2010). However, the molecular link between Rab35 and EHD1 remained unknown. In the present study, we discovered that two distinct Rab35 effectors, MICAL-L1 and centaurin-β2, cooperatively regulate the perinuclear localization of EHD1 during NGF-induced neurite outgrowth of PC12 cells. Based on our findings, we propose the following mechanism to explain the functional relationship between Rab35 and EHD1: (1) Rab35 accumulates at perinuclear Arf6-positive endosomes in an NGF-dependent manner; (2) MICAL-L1 and centaurin-β2 are recruited to the same compartment through interaction with Rab35; and then (3) MICAL-L1 and centaurin-β2 cooperatively recruit EHD1 to the same compartment through a direct interaction with EHD1 and by inactivating Arf6, respectively (Fig. 9).

Our model, in which Rab35 recruits MICAL-L1 to Arf6-positive endosomes, is consistent with our findings that Rab35 interacts with MICAL-L1 and that Rab35 and MICAL-L1 concomitantly accumulate at Arf6-positive endosomes in response to NGF stimulation. However, Rahajeng et al. have recently reported findings in regard to the relationship between Rab35 and MICAL-L1 that conflict with our model (Rahajeng et al., 2012). They showed that overexpression of active Rab35 in HeLa cells leads to dissociation of MICAL-L1 from tubular endosomes and that knockdown of Rab35 leads to association of MICAL-L1 with tubular endosomes. We do not know the exact reasons for these differences, but we suspect that they are attributable to the differences between the cell lines used and/or between the compartments on which the studies focused (i.e. tubular endosomes in HeLa cells versus perinuclear Arf6-positive endosomes in PC12 cells, although both are considered to be recycling endosomes). In any event, further work will be necessary to determine whether Rab35 functions as a positive

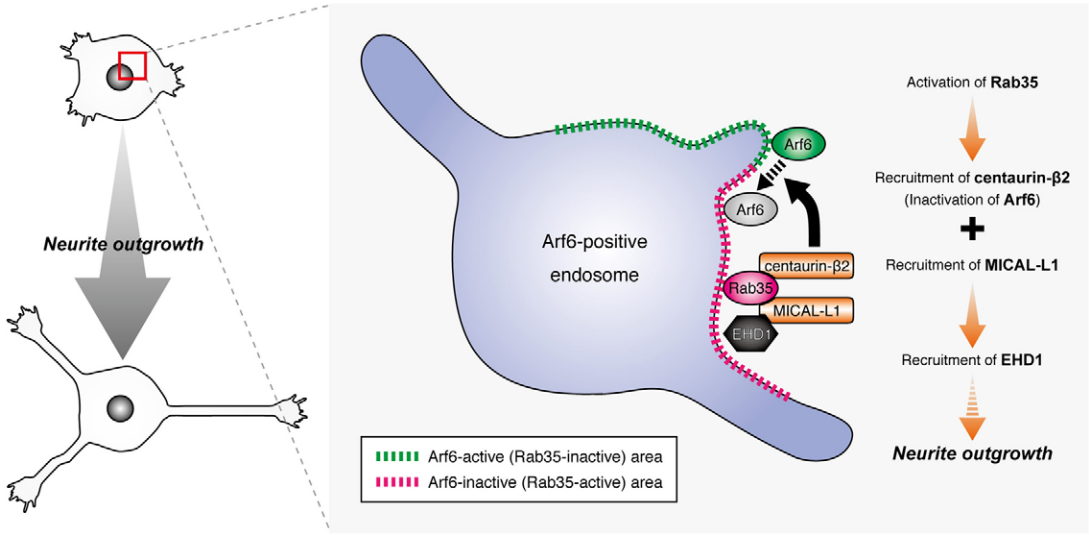

Fig. 9. A model of the molecular nexus consisting of endocytic recycling factors for successful neurite outgrowth. In response to NGF stimulation, Rab35 is first accumulated at the perinuclear Arf6-positive endosomes and subsequently recruits two distinct effectors, MICAL-L1 and centaurin-β2, to the same compartment (Figs 1–3). MICAL-L1 and centaurin-β2 function as a scaffold for EHD1 and as an inactivator of Arf6, respectively, and then cooperatively recruit EHD1 to the same compartment (Figs 5–7), which facilitates neurite outgrowth (Figs 4, 8).

regulator, a negative regulator, or both of MICAL-L1 by analyzing different cell lines and cellular events.

We previously reported finding that inactivation of Arf6 by Rab35 through centaurin-β2 is required for successful neurite outgrowth of PC12 cells (Kobayashi and Fukuda, 2012). The role of inactivation of Arf6 during neurite outgrowth, however, had remained unknown. In the present study, we showed that one role of inactivation of Arf6 by centaurin-β2 is to recruit EHD1 to the Arf6-positive endosomes. Since it had been proposed that active Arf6 induces loss of PtdIns4*P*, another scaffold factor for EHD1, on recycling endosomes (Caplan et al., 2002; Jović et al., 2009), because active Arf6 converts PtdIns4*P* to phosphatidylinositol 4,5-bisphosphate [PtdIns(4,5)P_2] by activation of an Arf6 effector, PtdIns4*P* 5-kinase (PIP5K) (Brown et al., 2001; Jović et al., 2009), it was speculated that inactivation of Arf6 might be required to maintain PtdIns4*P* and recruit EHD1. An important recent finding is that the PtdIns4*P*-producing enzyme PtdIns(4,5)P_2 5-phosphatase OCRL functions as a novel Rab35 effector during cytokinesis (Dambournet et al., 2011). These findings, together with our finding in the present study that Rab35 integrates the functions of MICAL-L1 and centaurin-β2, suggest that Rab35 functions as a quite efficient molecular switch for the formation of the EHD-association site on endosomes by bringing together two factors, MICAL-L1 and PtdIns4*P*, that are required to recruit EHD1.

There is one remaining question: how does EHD1 facilitate neurite outgrowth after its recruitment to Arf6-positive endosomes? EHD1 has been known to promote endocytic recycling, especially the trafficking from recycling endosomes to the plasma membrane by localizing at recycling endosomes (Naslavsky and Caplan, 2011). Since endocytic recycling has been proposed to be crucial to supplying membranes and/or proteins to neurite tips to enable their outward growth (Sann et al., 2009), EHD1 may facilitate this process by facilitating fission of vesicles that target to neurite tips from recycling endosomes in response to activation of Rab35 during neurite outgrowth.

In summary, we have demonstrated that Rab35 recruits and coordinates two distinct effector molecules, MICAL-L1 and centaurin-β2, at Arf6-positive endosomes, thereby enabling successful recruitment of EHD1 to the same compartment for neurite outgrowth. Our findings reveal a well-orchestrated molecular link between molecular switch Rab35 and molecular scissors EHD1 mediated by the coordination of the two distinct Rab35 effectors. This novel molecular nexus consisting of endocytic recycling factors, i.e. Rab35, centaurin-β2, Arf6, MICAL-L1 and EHD1, is crucial for successful neurite outgrowth.

Materials and Methods

Antibodies

The anti-Rab35 antibody and anti-centaurin-β2 antibody were prepared as described previously (Kobayashi and Fukuda, 2012). Anti-Arf6 mouse monoclonal antibody, anti-actin goat polyclonal antibody, anti-Myc tag mouse monoclonal antibody (Santa Cruz Biotechnology, Inc., Santa Cruz, CA), anti-MICAL-L1 mouse polyclonal antibody (Abnova, Taipei, Taiwan), anti-MICAL-L1 rabbit polyclonal antibody, anti-EHD1 rabbit polyclonal antibody (Abcam K.K., Tokyo, Japan), and anti-γ-tubulin mouse monoclonal antibody (Sigma-Aldrich Corp., St Louis, MO) were obtained commercially. Horseradish peroxidase (HRP)-conjugated anti-FLAG tag (M2) mouse monoclonal antibody (Sigma-Aldrich Corp.), HRP-conjugated anti-T7 tag mouse monoclonal antibody (Merck Biosciences Novagen, Darmstadt, Germany), HRP-conjugated anti-HA tag rabbit polyclonal antibody, HRP-conjugated anti-Myc tag mouse monoclonal antibody, and HRP-conjugated anti-red fluorescent protein antibody (MBL, Nagoya, Japan) were also obtained commercially. The Alexa-Fluor-488/594/633-conjugated secondary antibodies were from Invitrogen Corp. (Carlsbad, CA).

RNA interference

Double-stranded RNAs (siRNAs) targeted to rat *Rab35* (siRab35) and rat centaurin-β2 (siCentβ2) were prepared as described previously (Kobayashi and Fukuda, 2012). siRNAs targeted to rat *MICAL-L1* (siMICAL-L1, 19-base target site: 5′-CTGTAAGGAAGGCCACCAA-3′) was synthesized by Nippon EGT Corp., Ltd (Toyama, Japan). Short hairpin RNAs (shRNAs) targeted to rat *MICAL-L1* (shMICAL-L1 #1, 19-base target site: 5′-CTGTAAGGAAGGCCACCAA-3′ and shMICAL-L1 #2, 19-base target site: 5′-GACAAGATGTTGGAAACTA-3′) and rat *EHD1* (shEHD1 #1, 19-base target site: 5′-CAGGTTCATGTGTGCA-CAG-3′ and shEHD1 #2, 19-base target site: 5′-GCCCACCTATGATGAGATC-3′) were constructed as described previously (Kuroda and Fukuda, 2004), by using the pSilencer-neo 2.0-U6 vector (Ambion, Austin, TX), which expresses shRNA. Unless otherwise stated, shMICAL-L1 and shEHD1 mean shMICAL-L1 #1 and shEHD1 #1, respectively, throughout this paper. The knockdown by each siRNA

and shRNA was confirmed by its expression in PC12 cells for 48–60 hours followed by immunoblotting with specific antibodies as described below.

Plasmids

All mutant proteins used in this study are summarized visually in supplementary material Fig. S6. cDNAs encoding mouse Rab35, Rab35-Q67L, Rab35-S22N, centaurin-β2 (Centβ2-WT), centaurin-β2-R442Q (Centβ2-R442Q), centaurin-β2-ANKR (Centβ2-ANKR) and Arf6-Q67L were prepared as described previously (Kanno et al., 2010). Addition of the plasma membrane-targeting sequence (C-terminal 17 amino acids of mouse K-Ras; KDGKKKKKKSKTKCVIM) (Hancock et al., 1991) to the C terminus of Rab35 (Rab35–CAAX) and to the C terminus of Arf6 (Arf6–CAAX) was performed by a conventional PCR technique. cDNA encoding mouse MICAL-L1/mKIAA1668 was obtained from Kazusa DNA Research Institute (Chiba, Japan). MICAL-L1-CH (amino acids 1–113), MICAL-L1-LIM (amino acids 114–257), MICAL-L1-NPF (amino acids 258–658), MICAL-L1-CC (amino acids 659–870), and MICAL-L1-ΔCC (amino acids 1–658) were constructed by using a conventional PCR technique and the following pairs of oligonucleotides with a restriction enzyme site (underlined: *Bgl*II or *Bam*HI) or a stop codon (in bold): 5′-AGATCTATGGC-GGGGCCGCGGGGC-3′ (Met primer, sense) and 5′-**TCA**AGCTT-GGCCAGAACTGGT-3′ (CH reverse primer, antisense) for MICAL-L1-CH; 5′-AGATCTGCTGCCTCACCACCCAAA-3′ (LIM forward primer, sense) and 5′-**TCA**CACACTCAGGCTTGGGTC-3′ (LIM reverse primer, antisense) for MICAL-L1-LIM; 5′-AGATCTGCTGCAGTGGCTGAGGCA-3′ (NPF forward, sense) and 5′-**TTA**GGTGGCCTTCCTTACAGT-3′ (NPF reverse primer, antisense) for MICAL-L1-NPF; 5′-GGATCCAAAGGAGCCAAGCCT-3′ (CC forward primer, sense) and 5′-**TCA**GCTCTTGTCCCCTGG-3′ (Stop primer, antisense) for MICAL-L1-CC; and 5′-AGATCTATGGCGGGGCCGCGGGGC-3′ (Met primer, sense) and 5′-**TTA**GGTGGCCTTCCTTACAGT-3′ (NPF reverse primer, antisense) for MICAL-L1-ΔCC. MICAL-L1-ΔNPF, which has mutations in the first NPF (Asn-Pro-Phe) motif to APA (Ala-Pro-Ala), was constructed by using a PCR sewing technique and the following mutagenic oligonucleotides: 5′-TTCCTCAGCGGGGGCGTAGGGCTTGGG-3′ (ΔNPF reverse primer, antisense) and 5′-CCCAAGCCCTACGCCCCCGCTGAGGAA-3′ (ΔNPF forward primer, sense) essentially as described previously (Kobayashi and Fukuda, 2012). cDNA encoding mouse EHD1 was amplified from mouse brain Marathon-Ready cDNA (Clontech-Takara Bio Inc., Shiga, Japan) by using a conventional PCR technique and the following pairs of oligonucleotides with a *Bam*HI site (underlined) or a stop codon (in bold): 5′-GGATCCATGTTCAGCTGGGTGAGC-3′ (Met primer, sense) and 5′-**TCA**CTCGTGCCTCCCGTTT-3′ (stop primer, antisense). EHD1-EH (amino acids 401–534) was constructed by using a conventional PCR technique and the following pairs of oligonucleotides with a *Bam*HI site (underlined) or a stop codon (in bold): 5′-GGATCCGAGTCCCTGATGCCCTCA-3′ (EH forward primer, sense) and 5′-**TCA**CTCGTGCCTCCGTTT-3′ (Stop primer, antisense). EHD1-EH-K483E and EHD1-EH-W485A, which have point mutations of Lys 483 to Glu and Trp 485 to Ala, were constructed using a PCR sewing technique and the following mutagenic oligonucleotides: 5′-CTTCCAGATCTCCCCCAGCAC-3′ (K483E reverse primer, antisense), 5′-GTGCTGGGGGAGATCTGGAAG-3′ (K483E forward primer, sense), 5′-TGCCAACTTTGCGATCTTCCC-3′ (W485A reverse primer, antisense), and 5′-GGGAAGATCGCAAAGTTGGCA-3′ (W485A forward primer, sense), essentially as described previously (Kobayashi and Fukuda, 2012). The resulting cDNAs were inserted into a pEGFP-C1 vector (Clontech-Takara Bio Inc.), pmStr-C1 vector, or pMyc-C1 vector (Kobayashi and Fukuda, 2012) to identify subcellular localizations and/or for neurite outgrowth assays. The resulting cDNAs were inserted into the pEF-FLAG vector, pEF-T7 vector (Fukuda et al., 1999), pEF-HA vector (Fukuda, 2002), or pEF-Myc vector (Kobayashi and Fukuda, 2012) for use in the co-immunoprecipitation assays. Arf6 cDNAs were inserted into a pmStr-N1 vector (Kobayashi and Fukuda, 2012) and pHA-N1 vector, which was produced from the pmStr-N1 vector by replacing the mStr-coding sequence with a HA-tag-coding sequence, for use in identifying subcellular localizations. We performed DNA sequencing to confirm that no unexpected mutations had occurred in the open reading frame of the cDNAs described above.

Cell cultures and transfections

Culture of PC12 cells and COS-7 cells and plasmid and/or siRNA transfection into these cells were performed essentially as described previously (Kobayashi and Fukuda, 2012).

Immunoblotting

To evaluate the relative level of expression of Rab35, MICAL-L1, centaurin-β2, and EHD1 in PC12 cells, cells were harvested and homogenized with lysis buffer (50 mM HEPES-KOH, pH 7.2, 150 mM NaCl, 1 mM $MgCl_2$, 1% Triton-X-100, and protease inhibitors) as described previously (Fukuda and Kanno, 2005). The total cell lysates were analyzed by 10% SDS-PAGE followed by immunoblotting with specific primary antibodies. Immunoreactive bands were visualized with appropriate HRP-conjugated secondary antibodies (GE Healthcare Ltd, Little Chalfont, UK) and detected by enhanced chemiluminescence (ECL; GE Healthcare Ltd). The positions of the molecular mass markers (in kDa) are shown at the left of the immunoblotting data in the figures.

Co-immunoprecipitation and direct binding assays

Two days after transfection of plasmids, COS-7 were harvested and homogenized in the lysis buffer. Cell lysates expressing HA–MICAL-L1 were incubated for 1 hour at 4℃ with anti-HA-tag-antibody-conjugated agarose beads (Sigma-Aldrich Corp.; wet volume 10 µl). After washing the beads twice with 1 ml of washing buffer (50 mM HEPES-KOH, pH 7.2, 150 mM NaCl, 1 mM $MgCl_2$, 0.2% Triton X-100, and protease inhibitors), the beads coupled with HA–MICAL-L1 were incubated for 1 hour at 4℃ with cell lysate expressing FLAG–Rab35. After washing the beads three times with the washing buffer, the FLAG–Rab35 bound to the beads was analyzed by 10% SDS–PAGE followed by immunoblotting with HRP-conjugated anti-FLAG tag antibody. To achieve GTP (or GDP) loading (Fig. 1C), FLAG–Rab35 was incubated for 30 minutes at 4℃ with 50 mM HEPES-KOH, pH 7.2, 150 mM NaCl, and 5 mM EDTA for guanine nucleotide extraction, and then GTPγS (or GDP) and $MgCl_2$ were sequentially added to the solution to a final concentration of 0.5 mM (or 1 mM) and 10 mM, respectively, before the co-immunoprecipitation assays. To evaluate the effect of TBC1D10C (Rab35-GAP) on the interaction between Rab35 and MICAL-L1 (Fig. 1E), the beads coupled with HA–MICAL-L1 were incubated for 1 hour at 4℃ with cell lysate expressing FLAG–Rab35 alone or FLAG–Rab35 and T7–TBC1D10C. To evaluate the ability of Rab35 to form a complex with MICAL-L1 and centaurin-β2 (Fig. 1H), the beads coupled with HA–MICAL-L1-CC were incubated for 1 hour at 4℃ with cell lysate expressing T7–Centβ2-ANKR in the absence or presence of cell lysate expressing FLAG–Rab35-Q67L. To evaluate the ability of MICAL-L1-CC (or MICAL-L1-NPF) to disrupt the interaction between Rab35 (or EHD1) and MICAL-L1 (Fig. 4F; Fig. 8F), cell lysate expressing HA–MICAL-L1-CC (or HA–MICAL-L1-NPF) was added to the mixture of beads (anti-T7-tag-antibody-conjugated agarose beads; Merck Biosciences Novagen) coupled with T7–MICAL-L1 and cell lysate expressing FLAG–Rab35. To evaluate the ability of Rab35 to form a complex with EHD1 through MICAL-L1 (Fig. 6E), beads (anti-Myc-tag-antibody-conjugated Protein-G–Sepharose beads; GE Healthcare Ltd) coupled with Myc–EHD1 were incubated for 1 hour at 4℃ with cell lysate expressing FLAG–Rab35 in the absence or presence of cell lysate expressing HA–MICAL-L1. The immunoreactive bands were visualized by enhanced chemiluminescence (GE Healthcare Ltd). Input means 1/500 volume of the reaction mixture used for co-immunoprecipitation.

For direct binding assays (supplementary material Fig. S1), the beads coupled with T7–MICAL-L1-CC (or T7–Centβ2-ANKR) were washed twice with 1 ml of stripping buffer (50 mM HEPES-KOH, pH 7.2, 300 mM NaCl, 1 mM $MgCl_2$, 1% Triton X-100, and protease inhibitors) to remove co-immunoprecipitated proteins, which had been derived from COS-7 cells, from the beads. The beads coupled with T7–MICAL-L1-CC (or T7–Centβ2-ANKR) alone were incubated for 1 hour at 4℃ with purified GTP-loaded or GDP-loaded GST–Rab35 that had been prepared as described previously (Kanno et al., 2010). The bound proteins were visualized by staining with Coomassie Brilliant Blue R-250 (Wako Pure Chemical Industries, Ltd, Osaka, Japan). Input means 1/100 volume of the reaction mixture used for direct binding assays. The blots and gels shown in this paper are representative of at least three independent experiments.

Immunofluorescence and colocalization analyses

All of the procedures used to perform the immunofluorescence and colocalization analyses have been described elsewhere (Kobayashi and Fukuda, 2012). The results of the colocalization analyses are reported as means and standard deviation (s.d.; $n=30$ from three independent experiments for each colocalization analysis).

Quantification of the perinuclear signals of Rab35, MICAL-L1, centaurin-β2 and EHD1

Perinuclear signals were quantified essentially as described previously (Kobayashi and Fukuda, 2012). In brief, 54 hours after transfection of siRab35, siMICAL-L1 or siCentβ2, PC12 cells were treated with NGF for 6 hours. Cells were then fixed and stained with an antibody against Rab35, MICAL-L1, centaurin-β2, or EHD1 and fluorescence images of the transfected cells were captured at random under conditions in which none of the fluorescence signals was saturated. Then, because the Rab35, MICAL-L1, centaurin-β2 and EHD1 signals were especially concentrated around the centrosome in the perinuclear area, a 3 μm^2 area that contained γ-tubulin signals was selected as a region of interest (ROI), and the relative intensities of the fluorescence signals in the ROI were measured as perinuclear signals of Rab35, MICAL-L1, centaurin-β2 and EHD1 with the MetaMorph software. The perinuclear signal intensity of Rab35, MICAL-L1, centaurin-β2 or EHD1 in the control cells is expressed as 100 (arbitrary units, a.u.) in each experiment. The results of quantification are presented as means and standard error (s.e.m.; $n=60$ from three independent experiments for each quantification analysis).

Neurite outgrowth assays

Neurite outgrowth assays were performed essentially as described previously (Kobayashi and Fukuda, 2012). The results of the neurite outgrowth assays in this paper are reported as means and s.e.m. of one representative data from at least three independent experiments with similar results ($n>100$ from three dishes in each experiment).

Statistical analyses

Student's unpaired *t*-test was used to evaluate every result for statistical significance in comparison with the results obtained in control cells. The single asterisk (*) and double asterisk (**) in the bar charts indicate a *t*-test *P*-value of <0.05 and <0.01, respectively, and comparisons that yielded a *P*-value >0.05 are indicated by N.S. (not significant).

Acknowledgements

We thank Dr Takahiro Nagase for kindly donating the mKIAA1668 cDNA clone, Megumi Aizawa for technical assistance, and members of the Fukuda Laboratory for valuable discussions.

Author contributions

H.K. and M.F. conceived and designed the study; H.K. performed the experiments; H.K. and M.F. prepared the manuscript.

Funding

This work was supported in part by Grants-in-Aid for Scientific Research from the Ministry of Education, Culture, Sports, and Technology of Japan [grant numbers 24370077 and 24657125 to M.F.]; the Daiichi-Sankyo Foundation of Life Science (to M.F.); the Japan Society for the Promotion of Science (to H.K.) and the International Advanced Research and Education Organization of Tohoku University (to H.K.).

Supplementary material available online at
http://jcs.biologists.org/lookup/suppl/doi:10.1242/jcs.117846/-/DC1

References

Allaire, P. D., Marat, A. L., Dall'Armi, C., Di Paolo, G., McPherson, P. S. and Ritter, B. (2010). The Connecdenn DENN domain: a GEF for Rab35 mediating cargo-specific exit from early endosomes. *Mol. Cell* **37**, 370-382.

Barr, F. and Lambright, D. G. (2010). Rab GEFs and GAPs. *Curr. Opin. Cell Biol.* **22**, 461-470.

Brown, F. D., Rozelle, A. L., Yin, H. L., Balla, T. and Donaldson, J. G. (2001). Phosphatidylinositol 4,5-bisphosphate and Arf6-regulated membrane traffic. *J. Cell Biol.* **154**, 1007-1018.

Caplan, S., Naslavsky, N., Hartnell, L. M., Lodge, R., Polishchuk, R. S., Donaldson, J. G. and Bonifacino, J. S. (2002). A tubular EHD1-containing compartment involved in the recycling of major histocompatibility complex class I molecules to the plasma membrane. *EMBO J.* **21**, 2557-2567.

Chevallier, J., Koop, C., Srivastava, A., Petrie, R. J., Lamarche-Vane, N. and Presley, J. F. (2009). Rab35 regulates neurite outgrowth and cell shape. *FEBS Lett.* **583**, 1096-1101.

Dambournet, D., Machicoane, M., Chesneau, L., Sachse, M., Rocancourt, M., El Marjou, A., Formstecher, E., Salomon, R., Goud, B. and Echard, A. (2011). Rab35 GTPase and OCRL phosphatase remodel lipids and F-actin for successful cytokinesis. *Nat. Cell Biol.* **13**, 981-988.

de Curtis, I. (2001). Cell migration: GAPs between membrane traffic and the cytoskeleton. *EMBO Rep.* **2**, 277-281.

Donaldson, J. G. (2003). Multiple roles for Arf6: sorting, structuring, and signaling at the plasma membrane. *J. Biol. Chem.* **278**, 41573-41576.

Fukuda, M. (2002). Synaptotagmin-like protein (Slp) homology domain 1 of Slac2-a/melanophilin is a critical determinant of GTP-dependent specific binding to Rab27A. *J. Biol. Chem.* **277**, 40118-40124.

Fukuda, M. (2008). Regulation of secretory vesicle traffic by Rab small GTPases. *Cell. Mol. Life Sci.* **65**, 2801-2813.

Fukuda, M. and Kanno, E. (2005). Analysis of the role of Rab27 effector Slp4-a/granuphilin-a in dense-core vesicle exocytosis. *Methods Enzymol.* **403**, 445-457.

Fukuda, M., Kanno, E. and Mikoshiba, K. (1999). Conserved N-terminal cysteine motif is essential for homo- and heterodimer formation of synaptotagmins III, V, VI, and X. *J. Biol. Chem.* **274**, 31421-31427.

Fukuda, M., Kanno, E., Ishibashi, K. and Itoh, T. (2008). Large scale screening for novel rab effectors reveals unexpected broad Rab binding specificity. *Mol. Cell. Proteomics* **7**, 1031-1042.

Fukuda, M., Kobayashi, H., Ishibashi, K. and Ohbayashi, N. (2011). Genome-wide investigation of the Rab binding activity of RUN domains: development of a novel tool that specifically traps GTP-Rab35. *Cell Struct. Funct.* **36**, 155-170.

Grant, B. D. and Donaldson, J. G. (2009). Pathways and mechanisms of endocytic recycling. *Nat. Rev. Mol. Cell Biol.* **10**, 597-608.

Grant, B. and Hirsh, D. (1999). Receptor-mediated endocytosis in the *Caenorhabditis elegans* oocyte. *Mol. Biol. Cell* **10**, 4311-4326.

Hancock, J. F., Cadwallader, K., Paterson, H. and Marshall, C. J. (1991). A CAAX or a CAAL motif and a second signal are sufficient for plasma membrane targeting of ras proteins. *EMBO J.* **10**, 4033-4039.

Jackson, T. R., Brown, F. D., Nie, Z., Miura, K., Foroni, L., Sun, J., Hsu, V. W., Donaldson, J. G. and Randazzo, P. A. (2000). ACAPs are arf6 GTPase-activating proteins that function in the cell periphery. *J. Cell Biol.* **151**, 627-638.

Jović, M., Naslavsky, N., Rapaport, D., Horowitz, M. and Caplan, S. (2007). EHD1 regulates β1 integrin endosomal transport: effects on focal adhesions, cell spreading and migration. *J. Cell Sci.* **120**, 802-814.

Jović, M., Kieken, F., Naslavsky, N., Sorgen, P. L. and Caplan, S. (2009). Eps15 homology domain 1-associated tubules contain phosphatidylinositol-4-phosphate and phosphatidylinositol-(4,5)-bisphosphate and are required for efficient recycling. *Mol. Biol. Cell* **20**, 2731-2743.

Kanno, E., Ishibashi, K., Kobayashi, H., Matsui, T., Ohbayashi, N. and Fukuda, M. (2010). Comprehensive screening for novel Rab-binding proteins by GST pull-down assay using 60 different mammalian Rabs. *Traffic* **11**, 491-507.

Kobayashi, H. and Fukuda, M. (2012). Rab35 regulates Arf6 activity through centaurin-β2 (ACAP2) during neurite outgrowth. *J. Cell Sci.* **125**, 2235-2243.

Kouranti, I., Sachse, M., Arouche, N., Goud, B. and Echard, A. (2006). Rab35 regulates an endocytic recycling pathway essential for the terminal steps of cytokinesis. *Curr. Biol.* **16**, 1719-1725.

Kuroda, T. S. and Fukuda, M. (2004). Rab27A-binding protein Slp2-a is required for peripheral melanosome distribution and elongated cell shape in melanocytes. *Nat. Cell Biol.* **6**, 1195-1203.

Lin, S. X., Grant, B., Hirsh, D. and Maxfield, F. R. (2001). Rme-1 regulates the distribution and function of the endocytic recycling compartment in mammalian cells. *Nat. Cell Biol.* **3**, 567-572.

Maxfield, F. R. and McGraw, T. E. (2004). Endocytic recycling. *Nat. Rev. Mol. Cell Biol.* **5**, 121-132.

Montagnac, G. and Chavrier, P. (2008). Endosome positioning during cytokinesis. *Biochem. Soc. Trans.* **36**, 442-443.

Naslavsky, N. and Caplan, S. (2011). EHD proteins: key conductors of endocytic transport. *Trends Cell Biol.* **21**, 122-131.

Patino-Lopez, G., Dong, X., Ben-Aissa, K., Bernot, K. M., Itoh, T., Fukuda, M., Kruhlak, M. J., Samelson, L. E. and Shaw, S. (2008). Rab35 and its GAP EPI64C in T cells regulate receptor recycling and immunological synapse formation. *J. Biol. Chem.* **283**, 18323-18330.

Rahajeng, J., Giridharan, S. S. P., Cai, B., Naslavsky, N. and Caplan, S. (2012). MICAL-L1 is a tubular endosomal membrane hub that connects Rab35 and Arf6 with Rab8a. *Traffic* **13**, 82-93.

Sann, S., Wang, Z., Brown, H. and Jin, Y. (2009). Roles of endosomal trafficking in neurite outgrowth and guidance. *Trends Cell Biol.* **19**, 317-324.

Sato, M., Sato, K., Liou, W., Pant, S., Harada, A. and Grant, B. D. (2008). Regulation of endocytic recycling by *C. elegans* Rab35 and its regulator RME-4, a coated-pit protein. *EMBO J.* **27**, 1183-1196.

Scita, G. and Di Fiore, P. P. (2010). The endocytic matrix. *Nature* **463**, 464-473.

Sharma, M., Giridharan, S. S. P., Rahajeng, J., Naslavsky, N. and Caplan, S. (2009). MICAL-L1 links EHD1 to tubular recycling endosomes and regulates receptor recycling. *Mol. Biol. Cell* **20**, 5181-5194.

Shim, J., Lee, S. M., Lee, M. S., Yoon, J., Kweon, H. S. and Kim, Y. J. (2010). Rab35 mediates transport of Cdc42 and Rac1 to the plasma membrane during phagocytosis. *Mol. Cell. Biol.* **30**, 1421-1433.

Sorkin, A. and von Zastrow, M. (2009). Endocytosis and signalling: intertwining molecular networks. *Nat. Rev. Mol. Cell Biol.* **10**, 609-622.

Stenmark, H. (2009). Rab GTPases as coordinators of vesicle traffic. *Nat. Rev. Mol. Cell Biol.* **10**, 513-525.

van Ijzendoorn, S. C. D. (2006). Recycling endosomes. *J. Cell Sci.* **119**, 1679-1681.

Zerial, M. and McBride, H. (2001). Rab proteins as membrane organizers. *Nat. Rev. Mol. Cell Biol.* **2**, 107-117.

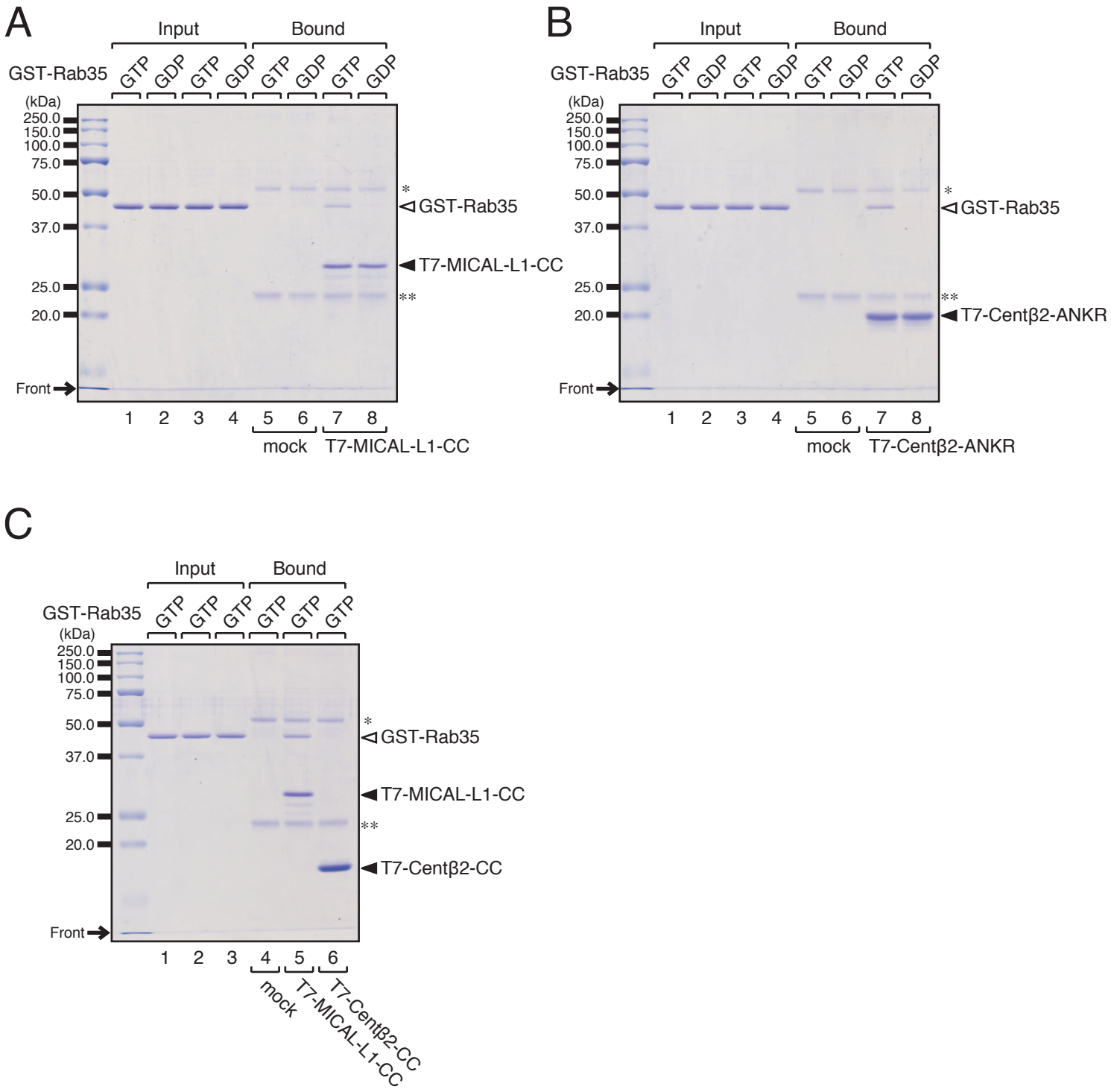

Fig. S1. MICAL-L1 and centaurin-β2 directly interact with active Rab35. (**A**) Direct interaction between GTP-bound Rab35 and MICAL-L1-CC. (**B**) Direct interaction between GTP-bound Rab35 and centaurin-β2-ANKR (Centβ2-ANKR). (**C**) GTP-bound Rab35 specifically interacts with MICAL-L1-CC, but not with Centβ2-CC. Beads coupled with T7-tagged proteins were washed with stripping buffer and then incubated with GST-tagged proteins. The bound proteins were visualized by staining with Coomassie Brilliant Blue R-250. The asterisks indicate the heavy chain (single asterisk) and light chain (double asterisk) of immunoglobulin G (anti-T7 tag antibody) used to conjugate T7-tagged proteins to the beads.

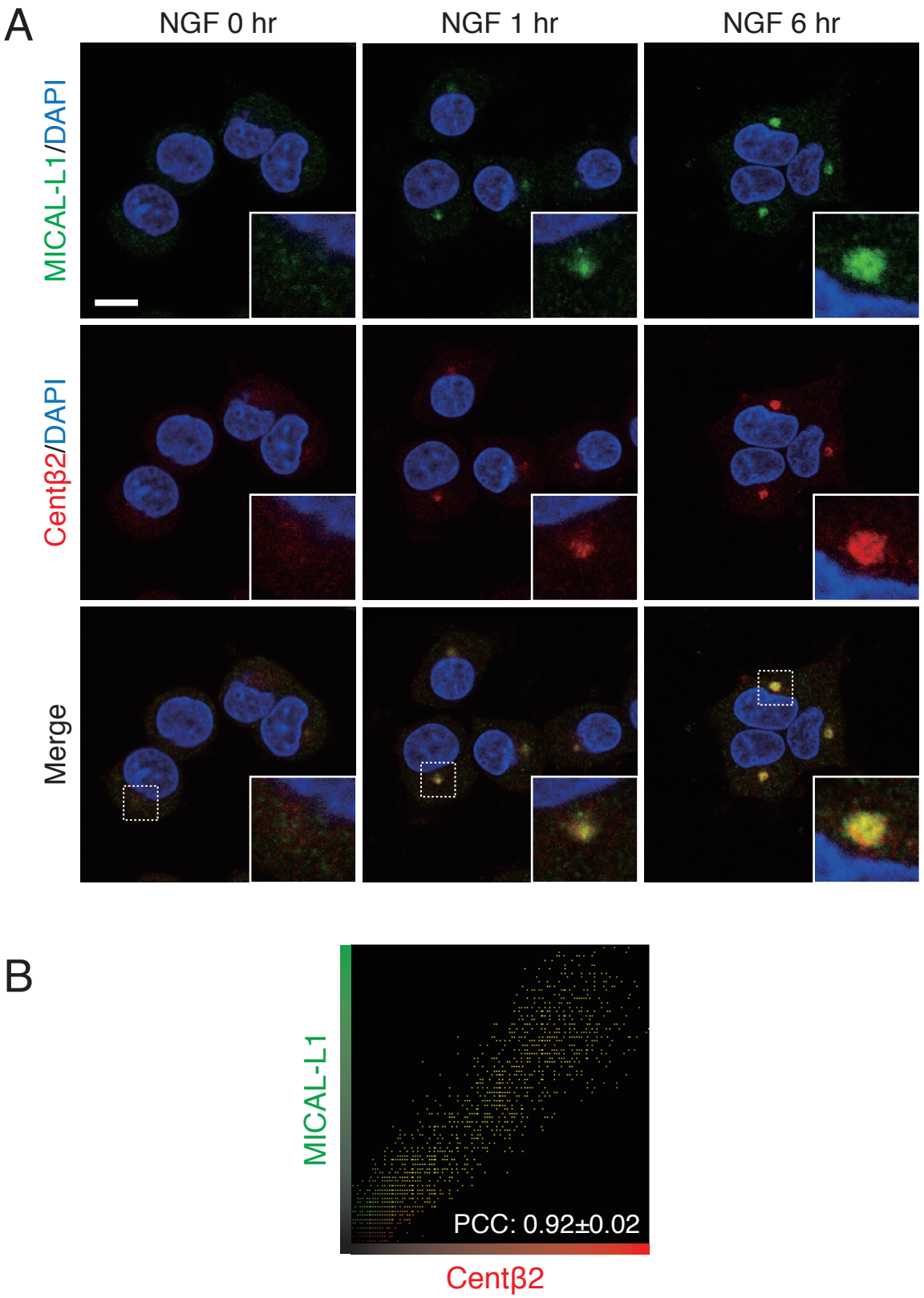

Fig. S2. MICAL-L1 and centaurin-β2 are concomitantly recruited to the perinuclear area in response to NGF stimulation. (**A**) Accumulation of MICAL-L1 and centaurin-β2 (Centβ2) in the perinuclear area of PC12 cells in response to NGF stimulation. After NGF stimulation for 0 hr (no NGF treatment), 1 hr, and 6 hr, PC12 cells were fixed and stained with anti-MICAL-L1 antibody, anti-Centβ2 antibody, and DAPI. The insets show magnified views of the boxed areas. Scale bars, 10 μm. (**B**) The intensity-scatter plot of MICAL-L1 signals versus Centβ2 signals in PC12 cells after NGF stimulation for 6 hr. The Pearson's Correlation Coefficient (PCC) value (mean ± SD) for the relation between them is shown at the bottom (n = 30 from 3 independent experiments).

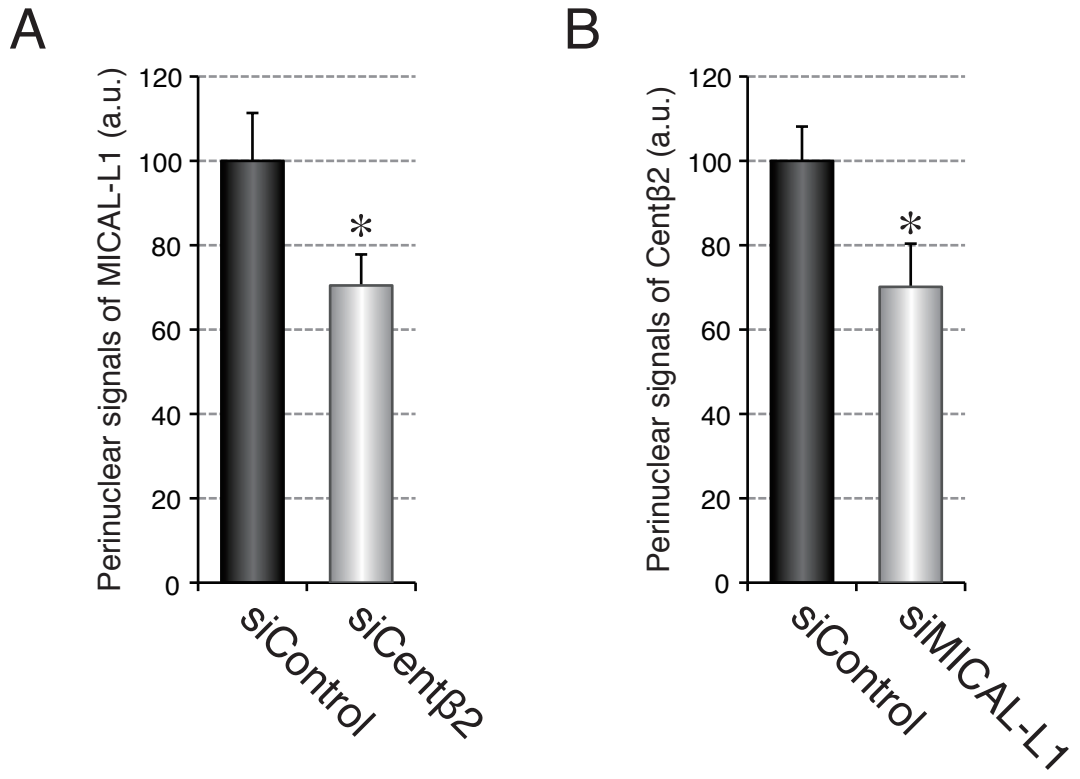

Fig. S3. MICAL-L1 and centaurin-β2 partially stabilize their perinuclear localization with each other. (**A**) Perinuclear MICAL-L1 signals (mean and SE; arbitrary units, a.u.) of siControl-treated and siCentβ2-treated PC12 cells (n = 60 from 3 independent experiments). (**B**) Perinuclear centaurin-β2 (Centβ2) signals (mean and SE; arbitrary units, a.u.) of siControl-treated and siMICAL-L1-treated PC12 cells (n = 60 from 3 independent experiments).

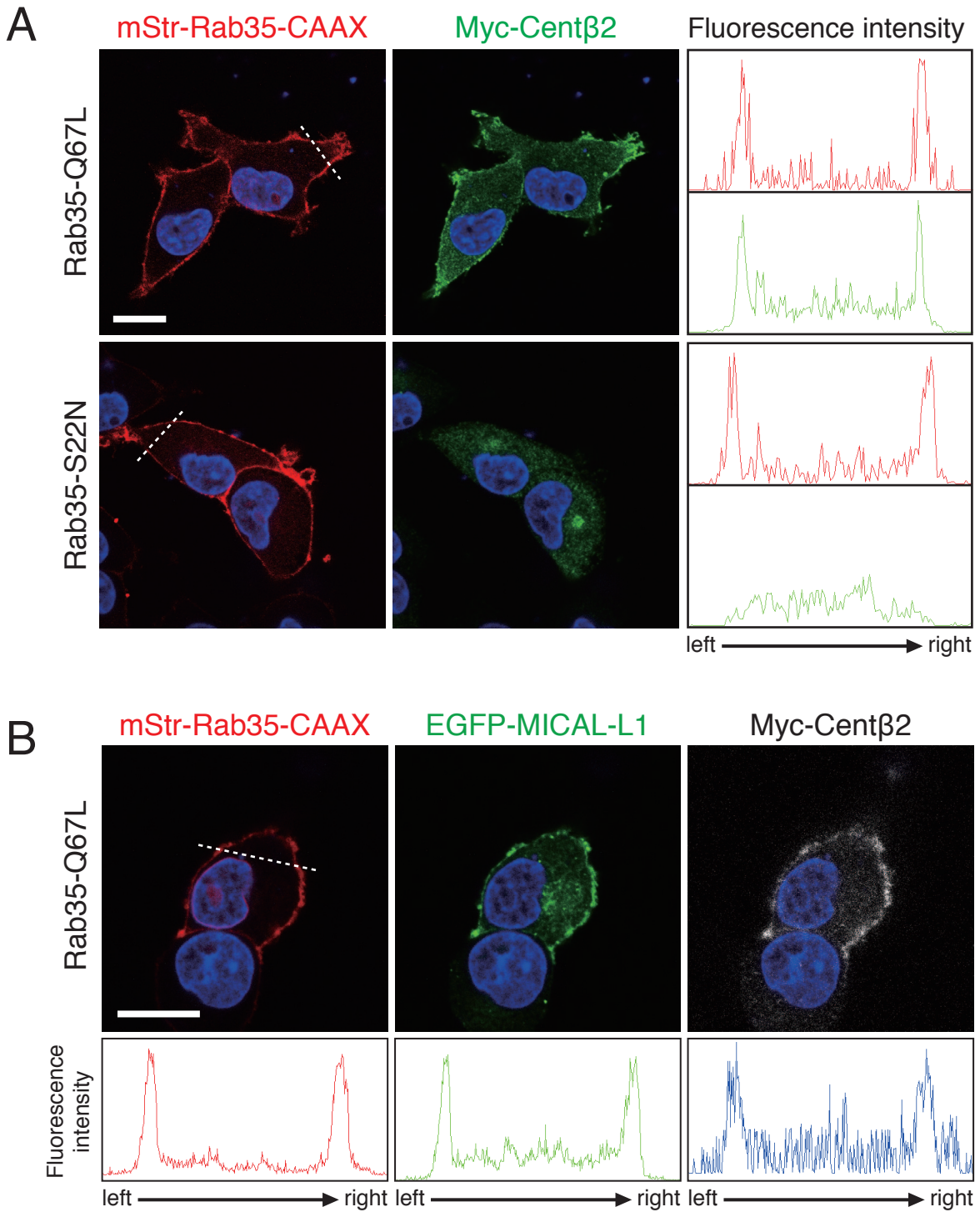

Fig. S4. Translocation of MICAL-L1 and centaurin-β2 to the plasma membrane in response to expression of plasma membrane-localized Rab35-Q67L–CAAX. (**A**) Translocation of centaurin-β 2 (Centβ2) to the plasma membrane in response to expression of plasma membrane-localized Rab35-Q67L–CAAX. PC12 cells transiently expressing Myc–Centβ2 together with either mStr–Rab35-Q67L–CAAX or mStr–Rab35-S22N–CAAX were fixed and stained with anti-Myc tag antibody and DAPI after NGF stimulation for 6 hr. (**B**) Translocation of MICAL-L1 and Centβ2 to the plasma membrane in response to expression of plasma membrane-localized Rab35-Q67L–CAAX. PC12 cells transiently expressing mStr–Rab35-Q67L–CAAX, EGFP–MICAL-L1, Myc–Centβ2 were fixed and stained with anti-Myc tag antibody and DAPI after NGF stimulation for 6 hr. Fluorescence intensity along the dashed lines is shown at the right (A) or the bottom (B). Scale bars, 10 μm.

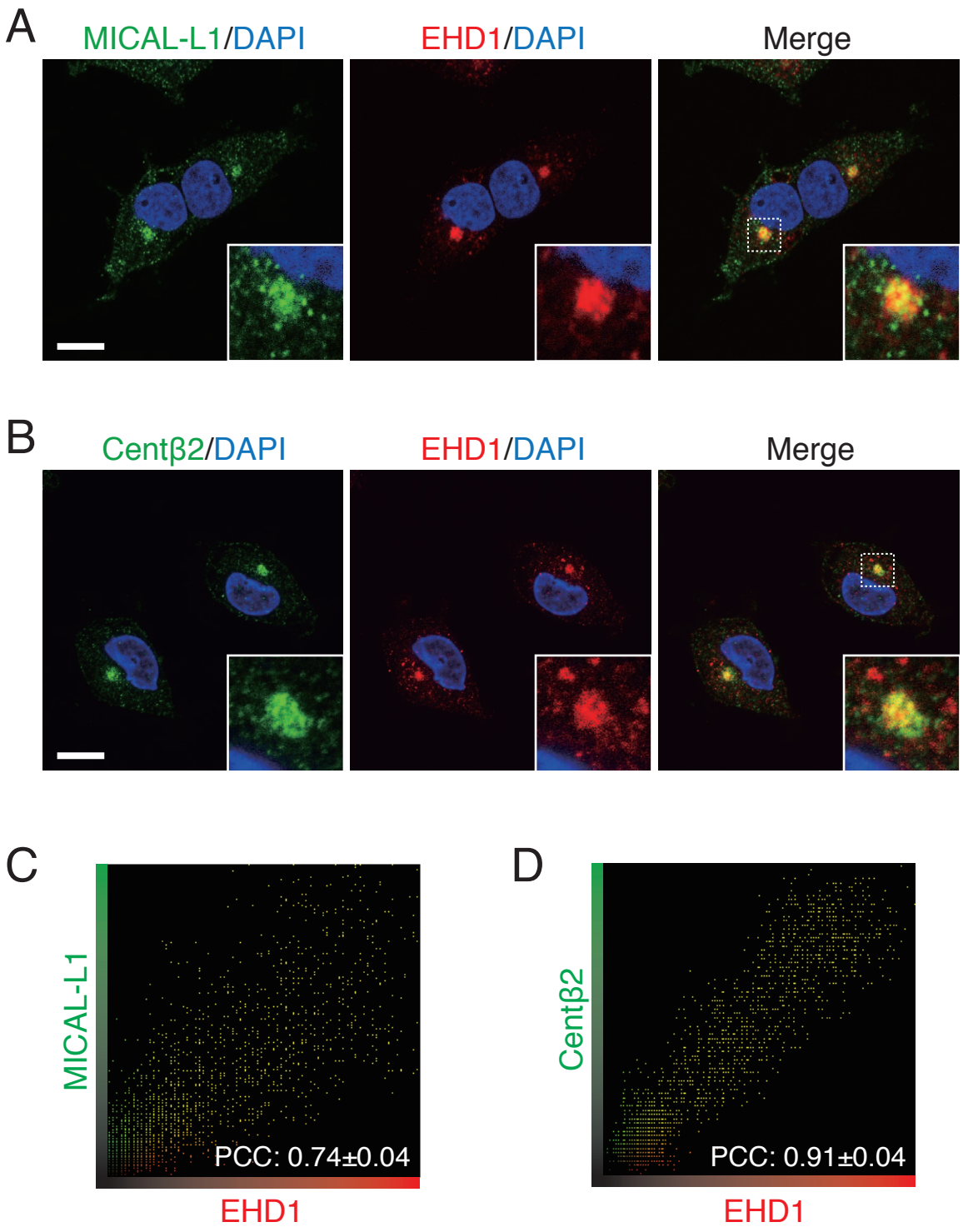

Fig. S5. MICAL-L1 and centaurin-β2 are colocalized with EHD1 in the perinuclear area. (**A**,**B**) PC12 cells were fixed and stained with anti-EHD1 antibody and DAPI together with anti-MICAL-L1 antibody (A) or anti-centaurin-β2 (Centβ2) antibody (B) after NGF stimulation for 6 hr. The insets show magnified views of the boxed areas. Scale bars, 10 μm. (**C**,**D**) The intensity-scatter plot of MICAL-L1 signals versus EHD1 signals (C), and Centβ2 signals versus EHD1 signals (D) in PC12 cells after NGF stimulation for 6 hr. The Pearson's Correlation Coefficient (PCC) value (mean ± SD) for the relation between them is shown at the bottom (n = 30 from 3 independent experiments).

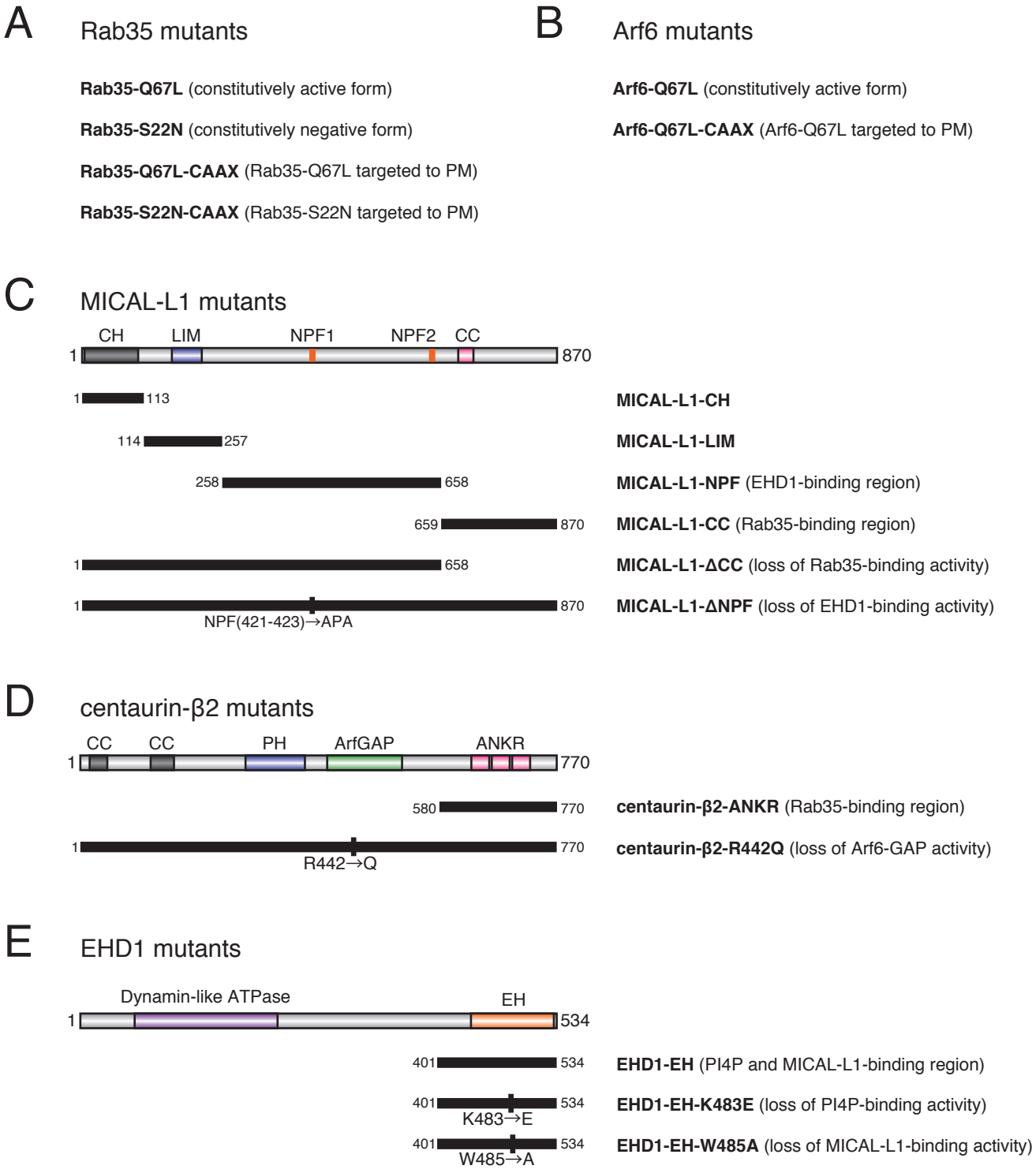

Fig. S6. Summary of the Rab35 mutants (A), Arf6 mutants (B), MICAL-L1 mutants (C), centaurin-β2 mutants (D), and EHD1 mutants (E) used in this study. Mutant names and their characteristic are shown.